doi:10.1038/nature19089

1. Supplementary Methods

1.1 Synthesis of nanoparticles

Synthesis of gold nanospheres. Gold nanoparticles with a spherical shape (nanospheres, NSs) with diameter of 19 ± 1 nm were synthesized using a two-step seed-mediated procedure reported elsewhere[1]. A seed solution was prepared by reducing $HAuCl_4$ (10 mL, 5×10^{-4} M) in 10 mL of aqueous citrate solution (5×10^{-4} M) *via* the addition of ice-cold solution of $NaBH_4$ in water (0.6 mL, 0.1 M) under stirring. The stirring was stopped 10 min after the addition of $NaBH_4$ solution, and the resultant solution was stored at room temperature for 2-3 h. A second solution, denoted as "Solution A" was prepared by dissolving $HAuCl_4$ (2.5×10^{-3} M) and cetyltrimethylammonium bromide (CTAB) (0.08 M) in water. An aqueous solution of ascorbic acid (0.5 mL, 0.1 M) was added to 9 mL of Solution A. Immediately after that, 10 mL of the aged seed solution was added to the above mixture under vigorous stirring. The resultant solution (Solution B) was stirred for 10 min and used 30 min after its preparation. Another solution, denoted as "Solution C", was prepared by dissolving $HAuCl_4$ (2.5×10^{-3} M) and CTAB (0.08 M) in water. An aqueous solution of ascorbic acid (0.5 mL of 0.1 M) was added to 9 mL of Solution C. Following this step, 9 mL of Solution B was added under vigorous stirring for 10 min. The resultant solution containing NSs was incubated at room temperature overnight.

Gold NSs with an average diameter of 40, 60 and 80 nm were obtained using a several-step procedure, including NS synthesis and subsequent etching. The latter step was used to produce NSs with close-to-spherical shape. Seed gold NSs were prepared using a method reported elsewhere[2,3]. A solution of freshly prepared, ice-cold $NaBH_4$ in deionized water (10

mM, 0.6 mL) was added under stirring to a solution prepared by mixing aqueous CTAB (0.1 M, 9.833 mL) and $HAuCl_4$ (15 mM, 0.167 mL) in a 20 mL scintillation vial, thereby forming a seed solution. After 2 min stirring, the pale yellow seed solution was left undisturbed at room temperature for 2 h. This solution was then diluted to 100 mL with deionized water. In another flask, growth solution was prepared by combining aqueous solutions of CTAB (0.24 M, 4 mL) with $HAuCl_4$ (15 mM, 0.133 mL) and ascorbic acid (0.1 M, 3 mL). The resulting clear solution was subsequently diluted to 50 mL with deionized water. To this solution, 0.6 mL of the diluted seed solution was added and the resulting mixture was shaken vigorously, resulting in a pale pink-coloured solution. The resultant solution was left undisturbed at room temperature for 12 h (to be used in the preparation of 40 nm-diameter NSs) or 30 min (prior to the preparation of 60 nm- and 80 nm-diameter NSs). Excess surfactant from this solution was removed by using one cycle of centrifugation (20,000 *g*, 20 min, 28 °C), removing the supernatant and redispersing NS seeds with deionized water. Later in the text, this solution is referred to as a "purified seed solution". To prepare 40, 60 and 80 nm-diameter NSs, 5, 2.5, or 1 mL of the purified seed solution, respectively, were added to a 20 mL scintillation vial and diluted it to 10 mL with deionized water. Then, 1.6 mL of aqueous surfactant solution (0.1 M CTAB for 40 nm-diameter NSs, 0.1 M cetylpyridinium chloride (CPC) for 60 nm and larger diameter NSs) was added to this solution. The resultant solution was heated to 30 ºC in a water bath for 5 min. The solution was removed from the water bath and 250 μL of 15 mM aqueous $HAuCl_4$ solution and 0.8 mL of 0.1 M ascorbic acid were added in succession. The NSs were left undisturbed at room temperature for 15 min. This synthesis was scaled up to obtain up to 500 mL of NS solution.

Gold NSs with a diameter in the range from 60 to 80 nm synthesized as described

above, did not have a spherical shape. To transform them into NSs, we used an etching procedure reported elsewhere[4]. Briefly, 10 mL of the as-synthesized NSs with a diameter of 60 or 80 nm NSs were purified from excess surfactant using centrifugation (5,000 *g*, 15 min, 28 °C), removal of the supernatant and dilution with deionized water. Equal volumes of the purified solution of gold NSs and 0.1M $FeCl_3$ were combined and left for 2 h at room temperature with intermittent stirring. The solution of NSs was then purified from excess reagents using two centrifugation cycles (5,000 *g*, 15 min, 28 °C), removal of the supernatant and dilution with an aqueous 50 mM CPC solution (5,000 *g*, 15 min, 28 °C), followed by the removal of the supernatant and addition of deionized water to achieve the original NS concentration. The resulting NSs exhibited a close-to-spherical shape.

Synthesis of spherocylindrical gold nanorods. Gold nanorods (NRs) were synthesized using the procedure reported elsewhere[5]. The seed solution was prepared by reducing $HAuCl_4$ (15 mM, 0.12 mL) in 2.5 mL of 0.2 M aqueous solution of CTAB with 0.6 mL of 10 mM cold $NaBH_4$. The seeds were aged for 30 min. To prepare the growth solution, a 10 mL aqueous solution of CTAB (8 mM) and sodium oleate (16 mM) was prepared in a 25 mL Erlenmeyer flask, followed by addition of 0.29 mL of 10 mM $AgNO_3$ solution. After 15 min of incubation at 30 °C, 10 mL of 1 mM $HAuCl_4$ solution was added, followed by stirring the mixture for 90 min at room temperature. At this point, 0.12 mL of concentrated HCl (12 M) was added to the growth solution, followed by addition of 1.25 mL of 0.064 M ascorbic acid. To initiate NR growth, 0.03 mL of the seed solution was added into the growth solution, which was stirred for 30 s and left undisturbed at 30 °C for 12 h. The resultant CTAB-stabilized NRs had an average diameter and length of 16 ± 1 nm × 80 ± 7 nm, respectively.

Synthesis of gold nanorods with a dumbbell shape. The preparation of gold nanoparticles with a dumbbell shape (NDs) was achieved by using a procedure described elsewhere[6]. CTAB (100 mM, 25 mL) was mixed with $HAuCl_4$ (50 mM, 0.125 mL) and stored for 5 min at 27 °C. Subsequently, KI (10 mM, 14.25 μL) and ascorbic acid (100 mM, 0.1 mL) were added. Finally, 0.6 mL of a solution of as-synthesized CTAB-functionalized spherocylindrical NRs (synthesized as described above) was used as a seed solution and was added to the mixture under stirring. After 15 min, the synthesis of NDs was complete. The resultant CTAB-stabilized NDs had a length of 92 ± 7 nm and the maximum diameter (measured at the ND tip) of 34 ± 2 nm and the minimum diameter (measured at the ND center) of 19 ± 2 nm.

Synthesis of silver nanocubes. Core-shell silver nanocubes (NCs) with a gold core (later in the text referred to as silver NCs) were stabilized with CPC and prepared using a three-step protocol reported elsewhere[7]. First, 3 nm-diameter gold NSs were prepared by rapidly injecting 0.60 mL of ice-cold, freshly prepared 10 mM $NaBH_4$ solution into a rapidly stirred mixed aqueous solution of $HAuCl_4$ (10 mM, 0.25 mL) and CTAB (0.1 M, 9.75 mL). After stirring for 2 min, the solution was left undisturbed for 2 h and then diluted to 100 mL with deionized water. Then, 0.6 mL of this solution was added under stirring to a mixture of $HAuCl_4$ (0.2 mL, 10 mM), CTAB (4 mL, 0.2 M), ascorbic acid (3 mL, 0.1 M) and 43 mL of deionized water. The reaction mixture was left undisturbed at room temperature for 12 h, yielding a purple solution of octahedral gold nanoparticles (seeds) approximately 16 nm in diameter. Two washing cycles using centrifugation at 15,000 *g* for 15 min and separation of the supernatant were used to replace the surfactant-rich solution with deionized water. In the final step, 2.5 mL of the solution of gold seeds, 7.4 mL of deionized water and 1.6 mL of the

aqueous 0.1 M solution of CPC were mixed in a 20 mL vial placed in an oil bath at 60°C. This step was followed by the sequential addition of the aqueous solution of $AgNO_3$ (0.2 mL, 10 mM) and ascorbic acid (0.8 mL, 0.1 M) under stirring. After 1 h, the reaction mixture was cooled in an ice-bath. The resulting NCs with the average length of the side of 40 nm were washed twice *via* centrifugation at 8,000 *g* for 10 min, separation of the supernatant and redispersion in deionized water.

Synthesis of gold nanocubes. Gold NCs were synthesized using a modified seed-mediated method reported elsewhere[8]. A solution of freshly prepared, ice-cold $NaBH_4$ in deionized water (10 mM, 0.6 mL) was added under stirring to a solution prepared by mixing aqueous CTAB solutions (0.1 M, 9.835 mL) and $HAuCl_4$ (15 mM, 0.167 mL) in a 120 mL Erlenmeyer flask. After 2 min stirring, the pale yellow mixture was left undisturbed for 2 h at room temperature. This seed solution was then diluted to 100 mL with deionized water. In another flask, a growth solution was prepared by combining aqueous solutions of CTAB (0.24 M, 4 mL) with $HAuCl_4$ (15 mM, 0.133 mL) and ascorbic acid (0.1 M, 3 mL). The resulting clear solution was subsequently diluted to 50 mL with deionized water. To this solution, 0.6 mL of the diluted seed solution was added. The resulting mixture was vigorously shaken and then left undisturbed for 12 h at room temperature. Excess CTAB from this solution was removed by one centrifugation cycle (15500 *g*, 20 min, 27 °C), removing the supernatant and redispersing the nanoparticle precipitate in 50 mL of deionized water.

To prepare 50 and 60 nm-diameter NCs, 30 and 20 mL of the purified seed solution, respectively, was added to a 120 mL Erlenmeyer flask and diluted to 100 mL with deionized water. Then, 16 mL of 0.1 M CTAB was added to this solution. The resultant mixed solution was heated to 30 ºC in a water bath for 5 min. Following this step, the solution was removed

from the water bath and 2.5 mL of 15 mM aqueous $HAuCl_4$ solution and 8 mL of 0.1 M ascorbic acid were added in succession, under stirring for 5 min. The resulting NCs were left undisturbed at room temperature overnight.

1.2 Polymers

Thiol-terminated polystyrene. Thiol-terminated polystyrene (PS) synthesized by anionic polymerization was purchased from Polymer Source, Inc. (Dorval, Canada). In the present work, we used PS samples with two molecular weights, M_n=50,000 g/mol and polydispersity index of 1.06 (referred to as PS-50K) and M_n=29,000 g/mol and polydispersity index of 1.07 (referred to as PS-30K).

Thiol-terminated poly(4-vinyl pyridine). Thiol-terminated poly(4-vinyl pyridine) (PVP) was synthesized by anionic polymerization, as reported elsewhere[9]. The polymerization was carried out in a tetrahydrofuran (THF)/hexamethylphosphoric triamide (HMPT) mixture (186 mL of THF and 4 mL of HMPT) and initiated with 1,1-diphenyl-3-methylpentyllithium prepared by the reaction of *sec*-butyl lithium (9.75 mg) with diphenylethylene (27.4 mg). The monomer 4-vinyl pyridine (6.0 g) was added to the solution of initiator at -78 °C. Polymerization took place for 2 h at room temperature and was terminated by adding ethylene sulphide (10 mg). The molecular weight of PVP was M_n= 40,400 g/mol and a polydispersity index was 1.05.

Thiol-terminated poly(*N*-vinylcarbazole). Thiol-terminated poly(*N*-vinylcarbazole) with the molecular weight M_n=19,200 g/mol and a polydispersity index of 1.34 was received from the group of Prof. Krzysztof Matyjaszewski (Carnegie Mellon University). The polymer was synthesized by RAFT polymerization of *N*-vinylcarbazole in the presence of S-(2-Ethyl

propionate) O-ethyl xanthate[10,11] and subsequent aminolysis of the xanthate chain-end[12].

Thiol-terminated random copolymer poly(styrene-*co*-isoprene). Thiol-terminated random copolymer poly(styrene-*co*-isoprene) (PS-*co*-PI) with a molecular weight M_n=53,500 g/mol and a polydispersity index of 1.16 was purchased from Polymer Source (Dorval, Canada). The copolymer was prepared by the anionic copolymerization of styrene and isoprene. The polymerization was terminated by the addition of propylene sulfide.

Polystyrene. Polystyrene with a molecular weight M_n=50,000 g/mol and a polydispersity index of 1.06 was supplied by Alfa Aesar Corporation.

Table S1 summarizes polymers used in the present study, along with their molecular weights and polydispersity index (PDI) Polymer Source Inc.

Table S1. Polymers used in nanoparticle patterning and the self-assembly experiments

Polymer	Notation	M_n (g/mol)	PDI
Thiol-terminated polystyrene	PS-30K	29,000	1.07
Thiol-terminated polystyrene	PS-50K	50,000	1.06
Thiol-terminated poly(styrene-*co*-isoprene)	PS-*co*-PI	53,500	1.16
Thiol-terminated poly(vinyl-4-pyridine)	PVP	40,400	1.05
Thiol-terminated poly(vinyl carbazole)	PVK	19,200	1.34
Polystyrene	-	50,000	1.06

1.3 Functionalization of nanoparticles with polymer ligands

Functionalization of nanoparticles with thiol-terminated polystyrene ligands. The solutions of as-synthesized NPs were concentrated from 1.5 mL solution to approximately 30 μL using 15 min centrifugation at 27 °C (*see* Table S2 for centrifugation speed) and subsequent removal of the supernatant. The concentrated NP solution was sonicated for ~5 s and added to 1.5 mL of the dilute (below crossover concentration) solution of thiol-terminated polystyrene in THF (Table S2). The resulting solution was maintained undisturbed at room temperature overnight. Then, the NPs were separated from free (non-attached) PS *via* six-ten cycles of centrifugation of the solution (six in the case of silver NCs) (Table S2, 15 min, 20 °C), removal of the supernatant, and dilution of the solution with THF. Table S2 summarizes polymer concentration and centrifugation conditions used in the ligand exchange process.

Table S2. Solutions of thiol-terminated polystyrene and centrifugation conditions used for ligand exchange

Type of metal NPs	Molecular weight, M_n, of thiol-terminated PS (g/mol)	Concentration of thiol-terminated PS in THF (mg/mL)	Centrifugation speed (*g*)
20 nm gold NSs	30,000	0.12	20,000
20 nm gold NSs	50,000	0.20	20,000
40 nm gold NSs	30,000	0.24	7,000

40 nm gold NSs	50,000	0.47	7,000
60 nm gold NSs	50,000	0.50	6,000
80 nm gold NSs	50,000	0.60	5,000
Gold NCs	50,000	0.50 or 0.005	6,000
Silver NCs	50 000	0.50	5,000
Gold NDs	50 000	2.0	7,000
Gold NRs	50 000	0.55	6,000

To examine the effect of grafting density on polymer surface segregation, polymer adsorption was varied by changing the ratio of polymer molar concentration to the surface area of the NSs, $C_{PS/SA}$, in the ligand exchange procedure. The value of $C_{PS/SA}$, in units of mol/nm^2, was obtained as

$$C_{\mathrm{PS/SA}} = \frac{C_{\mathrm{PS}}}{\pi D^2 C_{\mathrm{NS}} N_{\mathrm{Av}}} \quad \text{(S1)},$$

where C_{PS} is the concentration of PS-50K (mol L^{-1}) in the solution, C_{NS} is the concentration of gold NSs in the solution, D is the average diameter of gold NS (determined by analyzing TEM images) and N_{Av} is the Avogadro number (N_{Av}= 6.022 x 10^{23} mol^{-1}). The concentration of NSs was determined by measuring their extinction in the solution in THF as $C_{NS} = A/\varepsilon l$, where A is the absorbance value, ε is the molar absorptivity of the NSs (L mol^{-1}cm^{-1}), and l is the path length (cm) (Table S3).

Table S3. Molar absorptivity of gold NSs with different diameters

NS diameter, *D* (nm)	Molar absorptivity, ε ($\times 10^7$ L mol^{-1} cm^{-1})	Reference
20	1.1	1
40	9.9	13
60	35	13
80	77	13

The grafting density of PS-50K on the surface of gold NSs was determined by thermogravimetric analysis (TGA). Temperature-weight loss curves were obtained under nitrogen atmosphere using an SDT Q600 TGA from TA Instruments. The temperature was ramped at a heating rate of 10 °C/ min from 50 to 800 °C. The onset temperature of PS degradation was ~380 °C, while the temperature of 50% mass loss of the polymer was ~420 °C, consistent with previously reported values[14]. Representative TGA traces are shown in Fig. S1.

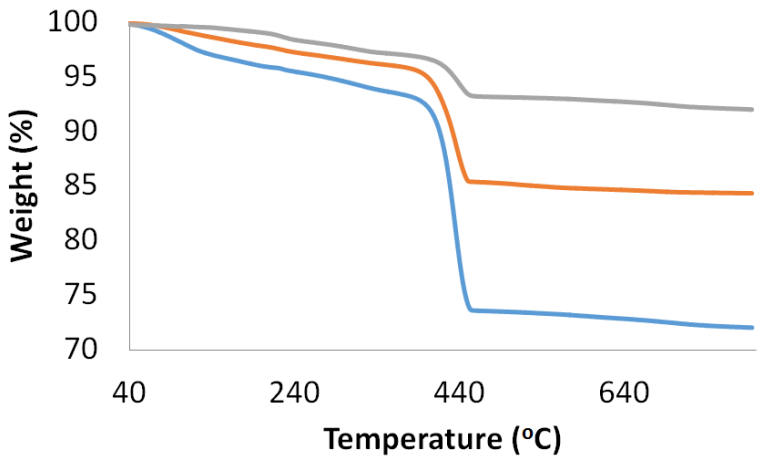

Figure S1. Representative thermal gravimetric analysis traces. Thermal gravimetric

analysis traces for 20 nm-diameter gold NSs stabilized with PS-50K. The ligand exchange procedure was conducted at the ratio of PS-50K concentration-to-NS surface area of 2.6×10^{-23} (blue trace), 2.6×10^{-24} (red trace) and 2.6×10^{-25} mol/nm^2 (grey trace).

Approximately 4-6 mg of PS-50K-capped gold NSs were analyzed in each experiment. The average grafting densities σ determined from two to four experiments for the different values of $C_{PS/SA}$ are summarized in Table S4. The grafting density of PS-50K was calculated using the method reported elsewhere[15] as

$$\sigma = \frac{\frac{4}{3}\left(\frac{wt_{shell}}{wt_{core}}\right)\rho_{core}\left(\frac{D}{2}\right)^3 N_{Av}}{M_n \pi D^2} \quad \text{(S2)},$$

where wt_{shell} and wt_{core} are the weight fractions (in %) of the polymer layer and the gold NSs, respectively, in the NS sample, determined by TGA, ρ_{core} is the density of gold[16] of 19.3 g cm^{-3}, and M_n is the molecular weight of PS ligands (M_n=50,000 g/mol).

Table S4. Variation in polymer grafting density with polymer concentration in the solution in ligand exchange process

NS diameter, D (nm)	Polymer concentration, $C_{PS/SA}$ (mol/nm^2)	Grafting density, σ (chains/nm^2)
20	3.0×10^{-23}	0.083 ± 0.0340
	3.0×10^{-24}	0.085 ± 0.0400
	3.0×10^{-25}	0.031 ± 0.0260

40	1.9×10^{-23}	0.042 ± 0.0019
	1.9×10^{-24}	0.031 ± 0.0015
	1.9×10^{-25}	0.012 ± 0.0086
	4.2×10^{-26}	0.003 ± 0.0010
60	2.4×10^{-23}	0.022 ± 0.0006
	2.4×10^{-24}	0.017 ± 0.0063
	2.4×10^{-25}	0.011 ± 0.0026
	2.4×10^{-26}	0.003 ± 0.0005
80	2.5×10^{-23}	0.029 ± 0.0028
	2.5×10^{-24}	0.021 ± 0.0057
	2.5×10^{-25}	0.012 ± 0.0058
	2.5×10^{-26}	0.004 ± 0.0021

* The standard deviation represent the average of two to four TGA measurements.

Functionalization of NSs with thiol-terminated poly(4-vinyl pyridine) ligands. The solution of as-synthesized 20 nm-diameter gold NSs was concentrated from 1.5 mL to approximately 30 μL using centrifugation (15,000 *g*, 30 min, 27 °C) and subsequent removal of the supernatant. The concentrated NS solution was sonicated for ~5 s and diluted with 15 mL of water. 1 mL of the NS solution was then dispersed in 10 mL of a dilute (below cross-over concentration) solution of thiol-terminated poly(4-vinyl pyridine) in DMF (2.5 mg/mL). The resulting solution was maintained undisturbed at room temperature overnight. Then, the NSs were separated from free poly(4-vinyl pyridine) *via* five cycles of centrifugation of the

solution (12,000 *g*, 15 min, 27 °C), removal of the supernatant, and dilution of the solution with DMF. The resulting solution of gold NSs in DMF (11 mL) was concentrated to 1 mL by centrifugation and dispersed in 10 mL of 0.01M HCl solution. The solution was purified by 2 cycles of centrifugation (12,000 *g*, 15 min, 27 °C), followed by NS redispersion in 0.01M HCl solution.

Functionalization of NSs with poly(*N*-vinyl carbazole). The solution of as-synthesized gold NSs was concentrated from 1.5 to ~30 μL using 15 min centrifugation at 27 °C (*see* Table S2 for centrifugation speed), and subsequent removal of the supernatant. The concentrated NS solution was sonicated for ~5 s and added to 1.5 mL of the 20 mg/mL solution of thiol-terminated poly(*N*-vinyl carbazole) dissolved in THF. The resulting solution was sonicated for 10 min and subsequently left undisturbed at room temperature overnight. Then, the NSs were separated from free poly(*N*-vinyl carbazole) *via* six cycles of 15 min-long centrifugation cycles at 20 °C at 20,000 *g*, removal of the supernatant, sonication and dilution of the solution with THF.

Functionalization of NSs with PS-*co*-PI copolymer. To remove excess CTAB, the solution of as synthesized 32 nm NSs in water (10 mL) was centrifuged (7,000 g, 15 min, 27 °C). After centrifugation, the supernatant was removed and the sediment was redispersed in 10 mL of deionized water. Subsequently, 10 mL of the NS solution were centrifuged (7,000 g, 10 min, 27 °C) and redispersed in 10 mL of 1 mg/mL solution of PS-*co*-PI in THF. After incubating the resulting solution for 18 h, the excess of unreacted PS-co-PI was removed by ten cycles of centrifugation (7,000 g, 10 min, 27 °C), each followed by the removal of supernatant and redispersion in 10 mL of THF.

Extinction spectra of polymer-stabilized gold NSs. Extinction spectra of the PS-stabilized NSs were acquired using a Cary 5000 UV-VIS-NIR spectrometer. Figure S2 shows extinction spectra for 20, 40, 60, and 80 nm- diameter gold NSs, all stabilized with PS-50K dispersed in THF. The extinction peaks red-shifted with increasing NS diameter.

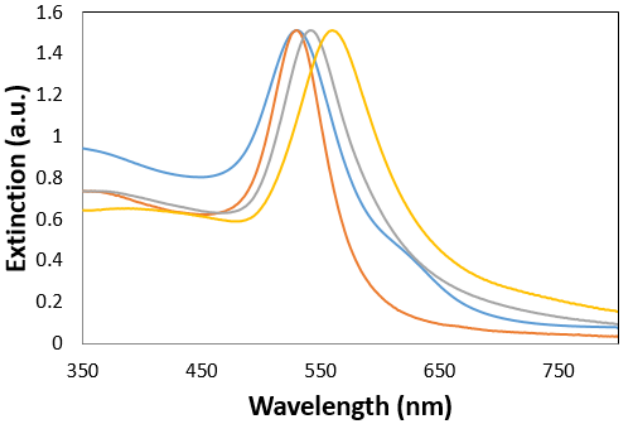

Figure S2. Extinction spectra of gold nanospheres. Extinction spectra of 20 (blue), 40 (red), 60 (grey), and 80 (yellow) nm-diameter gold NSs, all stabilized with PS-50K and dispersed in THF. The intensities of the spectra were normalized to match the maximum peak intensity of the 20 nm gold NS, that is, to 1.51 a.u.

Electron microscopy characterization of polymer-capped nanoparticles. TEM images were obtained using a Hitachi S-7000 microscope at 75-100 kV with a filled liquid nitrogen cold trap. Samples for electron microscopy imaging were prepared by drop casting the solution onto carbon-coated 300 mesh copper grids. Images were taken in different areas of the grid.

Images of polymer-capped NSs deposited from their solution in THF are shown in Figs. S3–S4, respectively. Images of CTAB-stabilized NRs, NDs, and NCs drop-cast from their

solution in water are presented in Figs S5–S8, respectively. The insets in S5-S8 show the NPs coated with a uniform PS-50K shell and deposited on the grid from the solution in THF.

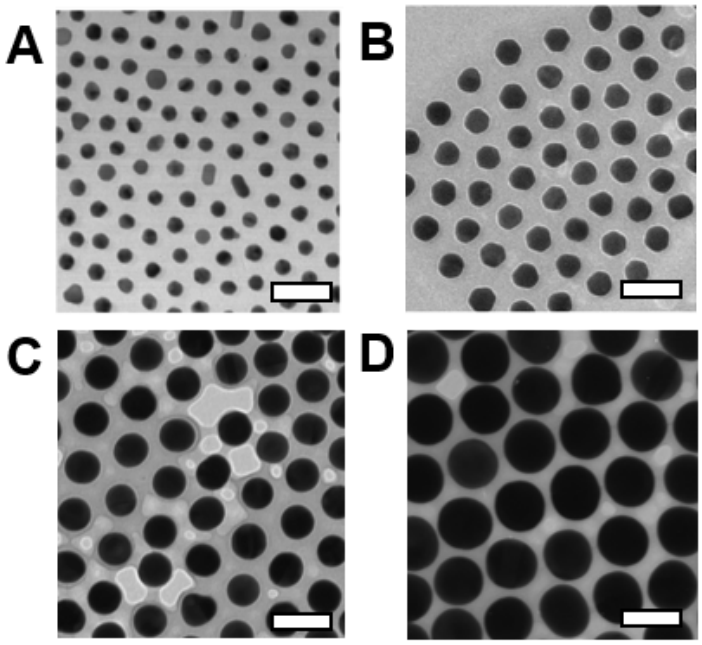

Figure S3. TEM images of gold nanospheres stabilized with PS-50K. Gold NSs tethered with PS-50K and deposited on a TEM grid from the solution in THF. Average NS diameters are 20 (**A**), 40 (**B**), 60 (**C**), and 80 nm (**D**). Scale bars are 100 nm.

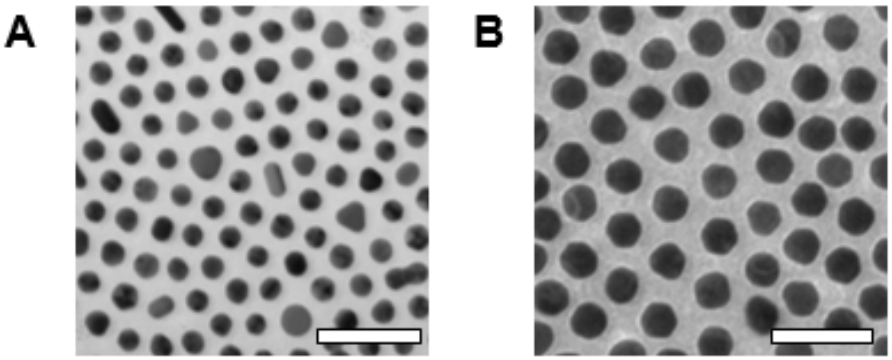

Figure S4. TEM images of gold nanospheres stabilized with PS-30K. Gold NSs capped with PS-30K and deposited on a TEM grid from the solution in THF. Average NS diameters are 20 (**A**) and 40 nm (**B**). Scale bars are 100 nm.

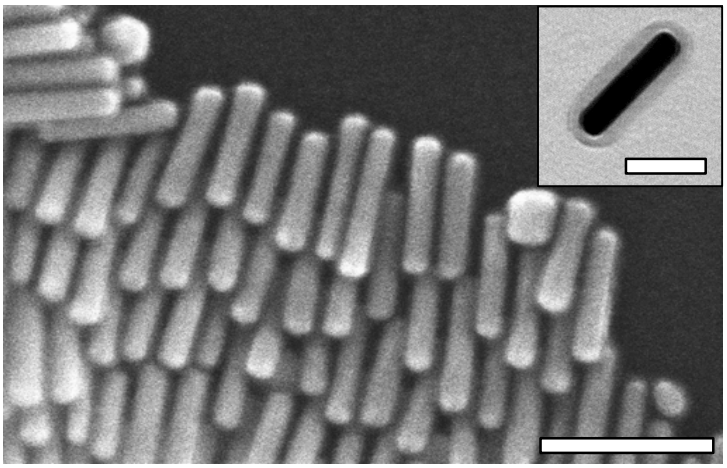

Figure S5. Electron microscopy images of gold nanorods. SEM image of gold NRs stabilized with CTAB and deposited on a TEM grid from the solution in water. Scale bar is 100 nm. Inset: TEM image of gold NRs stabilized with PS-50K, following ligand exchange. Scale bar is 50 nm.

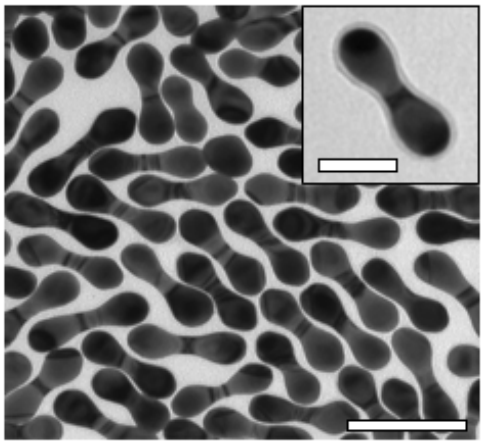

Figure S6. TEM images of gold nanodumbbells. TEM image of gold NDs stabilized with CTAB and deposited on a TEM grid from the solution in water. Scale bar is 100 nm. Inset:

TEM image of gold ND stabilized with PS-50K, following ligand exchange procedure. Scale bar is 50 nm.

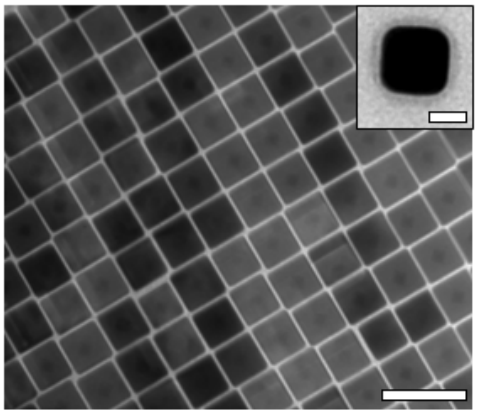

Figure S7. TEM images of silver nanocubes. TEM image of silver NCs stabilized by CTAB and deposited on a TEM grid from the solution in water. Scale bar is 100 nm. Inset: TEM image of silver NC stabilized with PS-50K, following ligand exchange procedure. Scale bar is 20 nm.

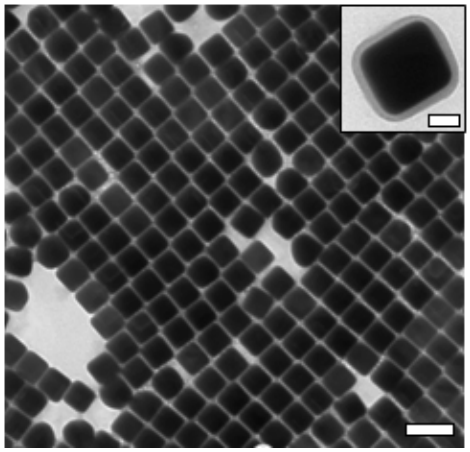

Figure S8. TEM images of gold nanocubes. TEM image of gold NCs stabilized by CTAB and deposited on a TEM grid from the solution in water. Scale bar is 100 nm. Inset: TEM

image of gold NC stabilized with PS-50K, following ligand exchange procedure. Scale bar is 20 nm.

1.4 Polymer surface segregation experiments

Sample preparation for imaging. To prepare samples of polymer-segregated NPs for TEM imaging, a droplet of the NP solution was deposited onto 300 mesh carbon-coated copper grids and left for 90 s unless otherwise specified. The remaining solution was removed with a Kimwipe tissue. TEM images were obtained using a Hitachi S-7000 microscope at 75-100 kV with a filled liquid nitrogen cold trap. Images were taken in different areas of the grid and typically, each experiment was repeated in triplicate with over 100 individual NP species imaged.

Polystyrene segregation on the surface of gold NSs. Polymer-capped NSs dispersed in THF were dried in a vial using a stream of air. Once the THF evaporated, the NSs were redispersed with 500 μL of DMF and sonicated for 5 s to prepare a 0.3 nM solution of gold NSs in DMF. To induce polymer segregation on the NS surface, water was added to the NS solution in DMF. To reduce the probability of the formation of kinetically trapped structures, water was added in a mixture with DMF, that is, 500 μL of a DMF/water mixture at C_w=8 vol. % to reach the total concentration of water in the solution of C_w=4 vol. %. The addition was carried out slowly, dropwise, and with careful and gentle mixing of the colloidal solution. Segregation experiments were carried out at an optimized temperature of 40 ^oC, in order to allow for an increased polymer flexibility. We note that further increase in the temperature to 80 ^oC did not show a noticeable effect of patch formation. The vial with a colloidal solution

was sealed and maintained in a water bath at 40 °C for 1-24 h, with no significant change in polymer surface structure for this time interval. Unless specified, the experiments were carried out for 24 h. Figures S9, S10, S12, and S13 show patches of PS-50K on the surface of 20, 40, 60, and 80 nm-diameter gold NSs. Figure S11 shows surface patches of PS-30K on 40 nm-diameter gold NSs.

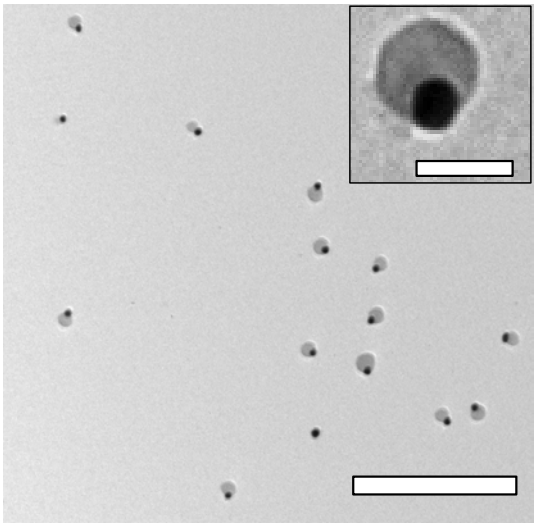

Figure S9. Polymer segregation on the surface of gold nanospheres. TEM image of 20 nm-diameter gold NSs stabilized with PS-50K. The NSs were incubated in the DMF-water mixture at C_w=4 vol. % for 24 h at 40 ^oC. Scale bar is 500 nm. Inset: Representative image of single-patch NS. Scale bar is 50 nm.

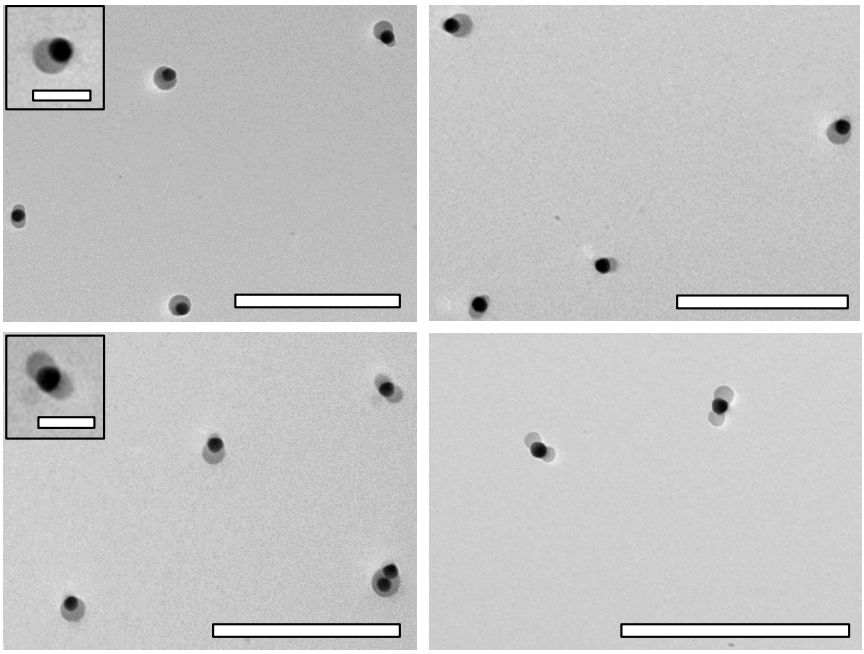

Figure S10. Polymer segregation on the surface of gold nanospheres. TEM images of 40 nm-diameter gold NSs stabilized with PS-50K. The NSs were incubated in the DMF-water mixture at C_w=4 vol. % for 24 h at 40 ^oC. Scale bars are 500 nm. Insets show representative single-patch (top) and two-patch (bottom) NSs. Inset scale bars are 50 nm.

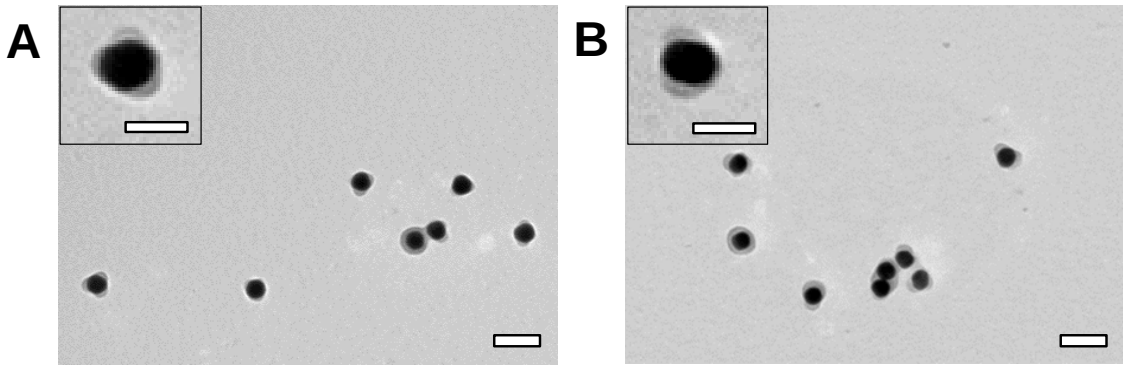

Figure S11. Polymer segregation on the surface of gold nanospheres. TEM images of 40 nm-diameter gold NSs stabilized with PS-30K. The NSs were incubated in the DMF-water mixture at C_w=4 vol. % for 24 h at 40 ^oC. Scale bars are 100 nm. Insets show representative three-patch (left) and two-patch (right) NSs. Scale bars are 50 nm.

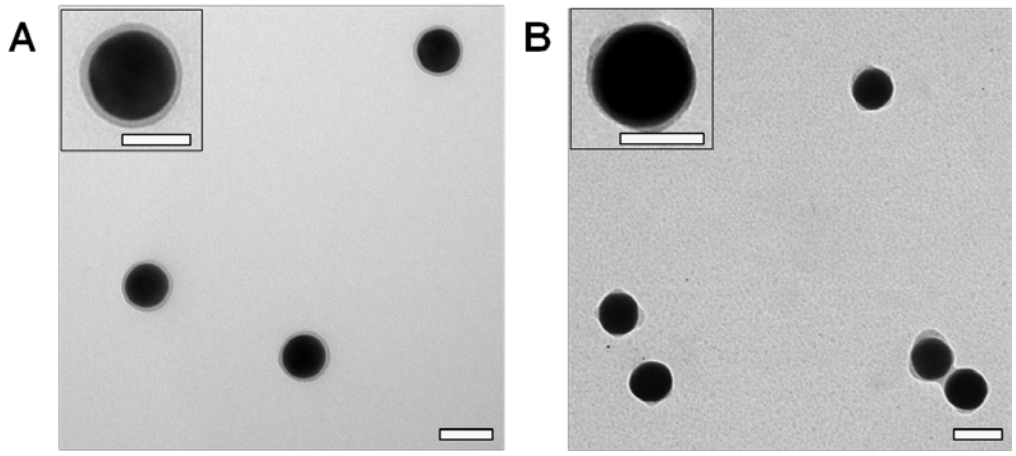

Figure S12. Effect of grafting density on polymer segregation on the nanosphere surface. (**A, B**) TEM image of 60 nm-diameter gold NSs stabilized with PS-50K with a grafting density of 0.03 (**A**) and 0.02 (**B**) chains/nm^2, both incubated for 24 h at 40 ^{o}C in the DMF-water mixture at C_w=4 vol. %. Scale bars are 100 nm. Inset: scale bars are 50 nm.

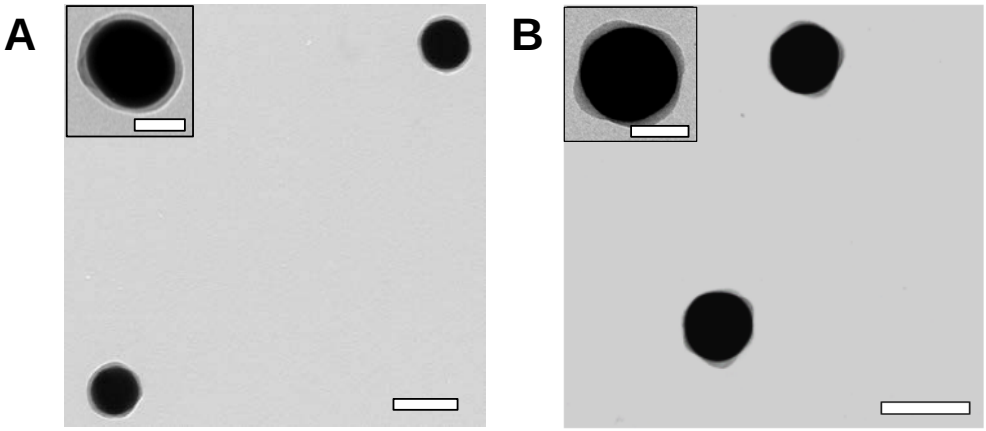

Figure S13. Effect of grafting density on polymer segregation on the surface of nanospheres. (**A, B**) TEM image of 80 nm-diameter gold NSs stabilized with PS-50K with a grafting density of 0.03 (**A**) and 0.012 (**B**) chains/nm^2, both incubated for 24 h at 40 ^{o}C in the DMF-water mixture at C_w=4 vol. %. Scale bars are 100 nm. Inset: scale bars are 50 nm.

Polystyrene segregation on the surface of non-spherical NPs. The solvent was evaporated from 100 μL of the as-prepared solution of PS-50K-capped silver NCs, gold NRs or gold NDs in THF. The NPs were redispersed in 250 μL of DMF and sonicated for 5 s. Then, 250 μL of a DMF/water mixture at C_w=8 vol. % was added dropwise to the NP solution in DMF under gentle swirling of the vial, to reach a resulting total water concentration of C_w=4 vol. %. The vial was sealed and maintained at 40 °C for 24 h (12 h for silver NCs). When gold NCs were used, the solvent was evaporated from 300 μL of the as-prepared solution of PS-50K-capped gold NCs in THF. The NPs were redispersed in 200 μL of DMF and sonicated for 5 s. A DMF/water mixture (200 μL at C_w=8 vol. %) was added dropwise to the NP solution in DMF under swirling of the vial, to reach a total water concentration of C_w=4 vol. %. The vial was sealed and maintained at 40 ° C for 24 h. Figures S14, S15, S16 and S17 show TEM images of patchy silver NCs, gold NCs, gold NRs and gold NDs, respectively.

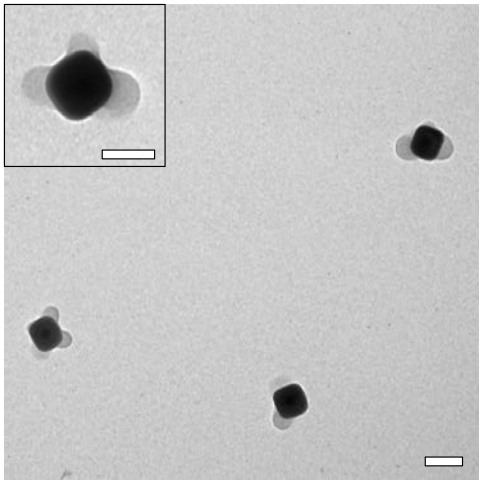

Figure S14. Polymer segregation on the surface of silver nanocubes. TEM images of

silver NCs stabilized with PS-50K and incubated in the DMF-water mixture at C_w=4 vol. % for 12 h at 40 ^oC. Inset shows an individual silver NC. Scale bars are 50 nm.

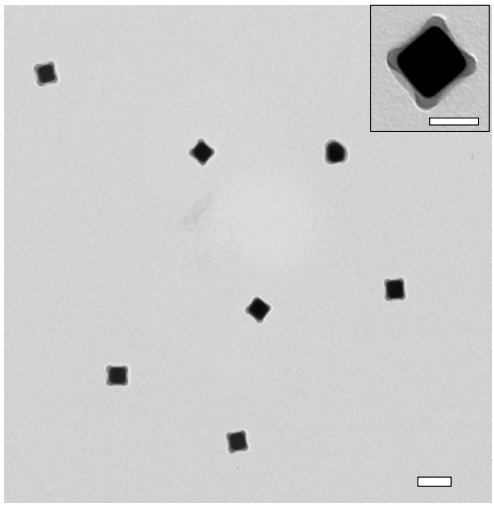

Figure S15. Polymer segregation on the surface of gold nanocubes. TEM image of gold NCs stabilized with PS-50K and incubated in the DMF-water mixture at C_w=4 vol. % for 24 h at 40 ^oC. Scale bar is 100 nm. Inset shows an individual gold NC. Scale bar is 50 nm.

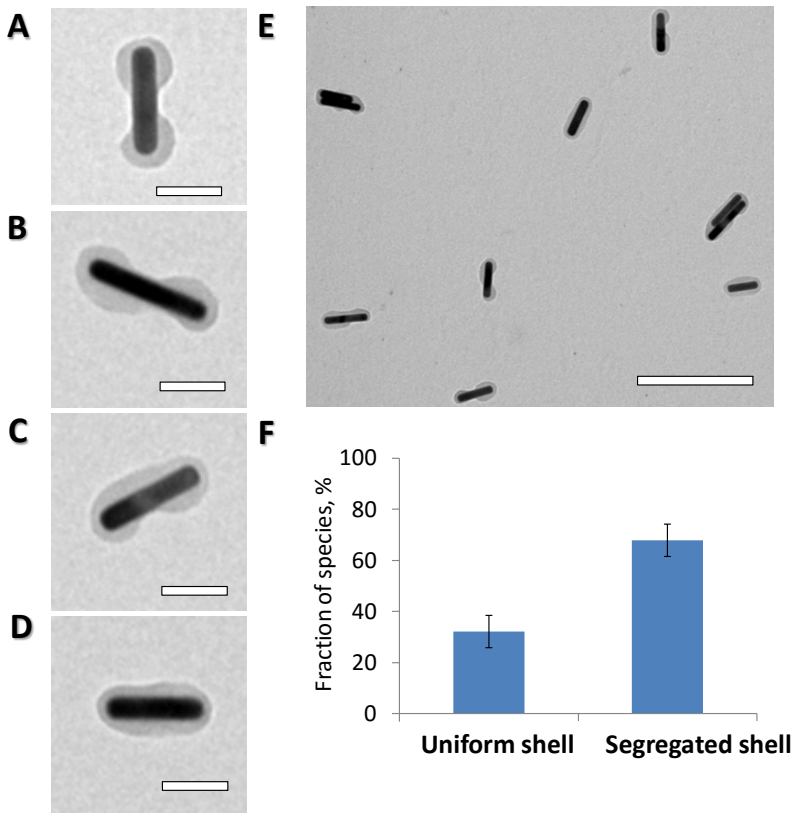

Figure S16. Polymer segregation on the surface of gold nanorods. **(A-D)** TEM images of spherocylindrical gold NRs stabilized with PS-50K and incubated in the DMF-water mixture at C_w=4 vol. % for 24 h at 40 ^oC. Scale bar is 100 nm. **(E)** TEM image of gold NRs shown in A-D. Scale bar is 500 nm. **(F)** Bar graph of the fractions of gold NRs with a uniformly-thick and surface-segregated PS layers. The data in (**F**) were collected from three experiments for 100 species in each experiment. Error bars represent the standard deviation.

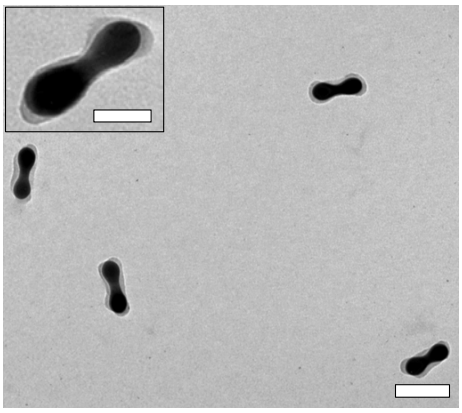

Figure S17. Polymer segregation on the surface of gold nanodumbbells. TEM image of gold NDs stabilized with PS-50K and incubated in the DMF-water mixture at C_w=4 vol. % for 24 h at 40 ^oC. Scale bar is 100 nm. Inset shows a representative image of an individual gold ND. Scale bar is 50 nm.

Polymer segregation experiments conducted in the THF-water solution on the surface of gold NCs. The solvent was evaporated from 300 μL of the as-prepared solution of PS-50K-capped gold NCs in THF. Ligand exchange was carried out from the 0.50 or 0.005 solution of PS in THF, followed by nine washing steps (centrifugation at 6,000 *g*, removal of the supernatant and redispersion in same initial amount of THF). Then, 250 μL of a THF/water mixture at C_w=8 vol. % was added dropwise to 250 μL of the solution of PS-50K-capped gold NCs in THF under gentle swirling of the vial, to reach the resulting C_w=4 vol. %. The NCs were redispersed in 200 μL of THF and sonicated for 5 s. The vial was sealed and maintained at 40 °C for 24 h. Figures S18 A and B show TEM images of patchy NCs formed under conditions described above and PS-50K-stabilized NCs after 24 h incubation in THF at 40 °C (control experiment).

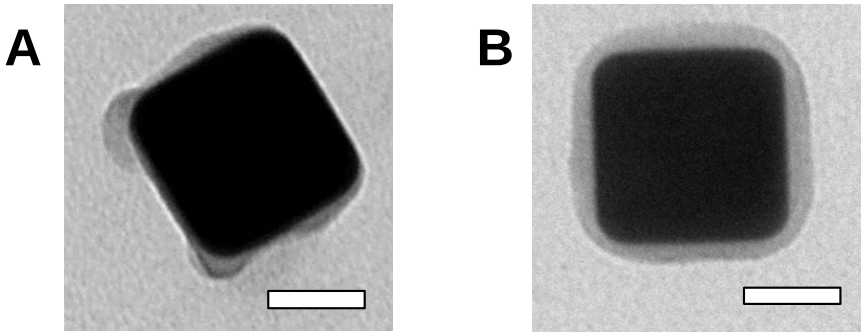

Figure S18. Polymer segregation on the surface of gold nanocubes in the THF-water mixture. (**A, B**) TEM images of gold NCs stabilized with PS-50K and incubated for 24 h at 40 ^{o}C in the THF-water mixture at C_w=4 vol. % (**A**) and in THF (control experiment) (**B**). Scale bars are 25 nm.

Polymer segregation on the surface of gold NSs functionalized with poly(*N*-vinyl carbazole). 25 μL of the solution of poly(*N*-vinyl carbazole)-functionalized 20 nm-diameter NSs in THF was dried and redispersed with 125 μL DMF. The solution was sonicated for ~5s before dropwise addition of 125 μL of a DMF-water mixture with C_w=4 vol. %. The final solution was incubated at 40 °C for 24 h. Figure S19A shows TEM images of poly(*N*-vinyl carbazole)-tethered NSs in the solution in DMF (control system) (left) and the NS displaying polymer surface segregation in the DMF-water mixture (right).

Polymer segregation on the surface of gold NSs functionalized with poly(4-vinyl pyridine). 100 μL of the solution of poly(4-vinyl pyridine)-functionalized 20 nm-diameter gold NSs in 0.01 M HCl was added to 900 μL of NaOH (~0.1 M). The final pH of the solution was 10.5. The solution was incubated at 40 °C for 24 h. Figure S19B shows TEM images of the controlled system at pH=2.5 (left) and a patchy NS at pH=10.5 (right).

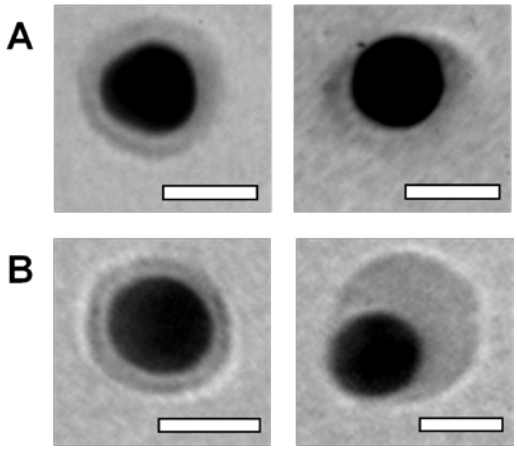

Figure S19. Surface segregation of polymer on the surface of gold nanospheres. **(A)** TEM image of a poly(*N*-vinyl carbazole)-capped gold NS deposited from DMF (left) and the DMF-water mixture at C_w=2 vol. % after 24 h incubation at 40 ° C (right). **(B)** TEM image of a poly(4-vinyl pyridine)-capped gold NS deposited from the aqueous acidic solution (pH=2.5), a good solvent for poly(4-vinyl pyridine) (left) and the aqueous basic solution (pH=10.5), a poor solvent for poly(4-vinyl pyridine) (right). The scale bars are 20 nm.

Crosslinking of PS-*co*-PI patches on gold NSs. To ensure that polymer surface segregation occurs in the solution and to show the ability to generate permanently segregated polymer surface pattern, we photocrosslinked the patches formed by PS-*co*-PI on the surface of gold NSs in the solution, that is, without drying them on a solid substrate. To induce polymer surface segregation on gold 35 nm-diameter NSs, a DMF/water solution (200 μL, C_w=2 vol. %) was added to 200 μL of the solution of PS-*co*-PI-functionalized gold NSs in DMF to obtain the final concentration of water of C_w=1 vol. %. The solution was sonicated for ~5 s and then immersed in a bath at 40 °C for 18 h to generate surface patches. Subsequently, 100 μL of the patchy NSs was added to 100 μL of a solution of azobisisobutyronitrile (AIBN) solution (0.1 wt. %) in the DMF/water mixture at C_w=1 vol. %.

The suspension was incubated at 4 °C for 4 h to allow AIBN to diffuse into the copolymer patches. Subsequently, the NS solution was exposed to ultra-violet illumination (UV-A lamp, Honle, UVAPrint 40C, λ=365 nm, I=30 mW cm^{-2}) for 5 min. Under these conditions, the AIBN radicals initiated crosslinking of the 3,4-polyisoprene units of the PI block. To demonstrate permanent crosslinking of the PS-*co*-PI patches, 100 μL of the resulting NS solution was diluted in 1 mL of THF, a good solvent for the PS-*co*-PI copolymer, sonicated for 15 min and incubated at room temperature for 24 h. Figure S20A and D show that the crosslinked patches were preserved under good solvency conditions. In the control experiments, 100 μL of the solution of patchy NSs functionalized with non-crosslinked PS-*co*-PI in DMF/water mixture (C_w=1 vol. %) was diluted with 1 mL of THF, sonicated for 15 min and incubated at room temperature for 24 h. Alternatively, the solution of patchy NSs was irradiated with ultra-violet light, diluted with 1 mL of THF to C_w=0.1 vol. %, sonicated for 15 min and incubated at room temperature for 24 h. In both cases, a large fraction of patchy NSs transformed into the core-shell NSs with a smooth, uniformly-thick shell **(**Figs. S20B and C).

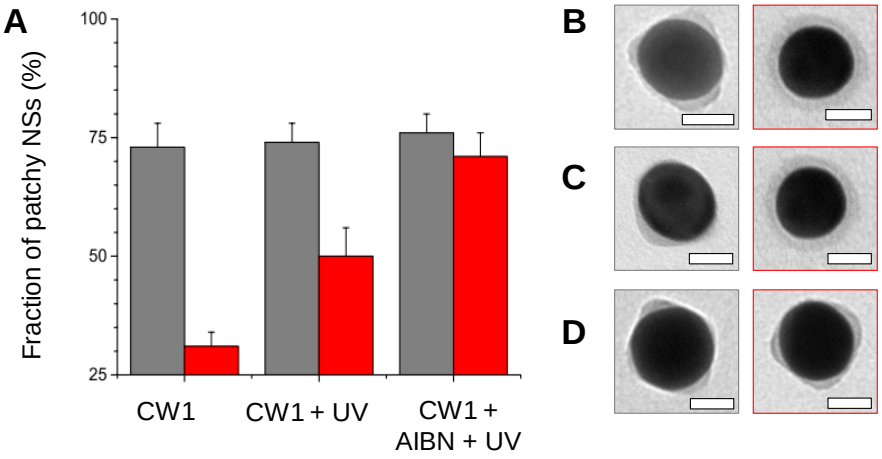

Figure S20. Segregation of the PS-*co*-PI copolymer on the surface of gold nanospheres. (**A**) The histogram depicts the fraction of patchy NSs in the original DMF/water solution at

C_w=1 vol. % (grey bars) and in solution diluted with THF to C_w=0.1 vol. % (red bars). From left to right: experiments conducted in the DMF/water solution at C_w=1 vol. % (labeled as CW1); experiments conducted in the DMF/water solution at C_w=1 vol. % exposed to irradiation (labeled as CW1 + UV) and experiments conducted in the DMF/water solution at C_w=1 vol. % with added AIBN under UV irradiation (CW1 + AIBN + UV). The fraction of patchy NSs was determined as the average of three experiments with approximately 40 NSs counted per experiment. The error bars represent the standard deviations. (**B**) TEM images of PS-*co*-PI-patterned NSs at C_w=1 vol. % before (left) and after (right) dilution with THF. (**C**) Representative TEM image of PS-*co*-PI-patterned NSs at C_w=1 vol. % subjected to UV irradiation in the DMF/water solution at C_w=1 vol. % before (left) and after (right) dilution with THF. (**D**) TEM image of PS-*co*-P-capped NSs in the DMF/water solution at C_w=1 vol. % subjected to UV irradiation in the presence of AIBN before (left) and after (right) dilution with THF. The colors of the frames in (**B-D**) correspond to bar colors in (**A**). Scale bars are 20 nm.

1.5 Tomography experiments

The low-dose bright-field TEM tilt series imaging of patchy gold NSs was conducted on a JEOL instrument with a LaB_6 emitter operated at 120 keV from -70 to +70 degrees with two-degree intervals with a total dosage of 40 electrons/Å^2. The tilt images were deliberately defocused by approximately one micrometer to increase contrast of the polymer patches. We performed a simple contrast flipping and deliberately turned off contrast transfer correction for image preparation for weighted back project. Due to the defocusing, all the boundaries of the polymer patches were outlined with a Fresnel fringe in the project images, as well as in the reconstruction. This Fresnel contrast helped identify the boundary of the polymer patches

when hand-segmenting them by tracing the Fresnel boundary of the low-intensity polymer in one cross-sectional image at a time.

The images were aligned using the center of mass of the NSs. The 3D data set was reconstructed using weight back projection and 3D visualization of the reconstructions was rendered by the Amira software. Importantly, the Fresnel fringes limited the sensitivity in detecting an ultrathin polymer layer on the surface of the NSs. The resolution of the reconstruction was estimated to be 2-3 nm.

Figure S21 shows the monochrome reconstructed image (top view) and 3D images of 60 nm-diameter gold NS with three PS-50K patches, each labeled with a different arbitrary color.

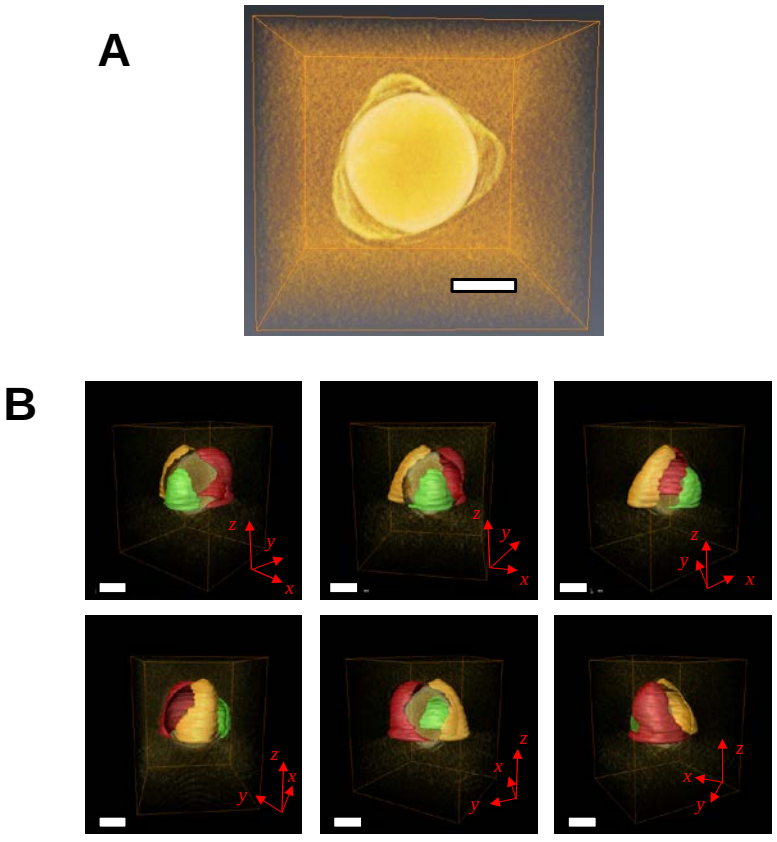

Figure S21. Reconstructed 3D images of 60 nm-diameter patchy nanospheres

functionalized with PS-50K. (**A**) Monochrome reconstructed image of gold NS with polymer patches (top view). (**B**) 3D images reconstructed from the TEM tilt series. The reconstructed gold core is removed for clarity of visualization of the polymer patches. From left to right, the images show the rotation of the NS around the axis normal to the plane of the TEM grid. Each patch is shown with a different color for their visual separation. The substrate is not visible on the reconstructions, due to its low electron density. Partial wetting of the substrate with a polymer is evident from the meniscus-like shape of the interface between the patches and the substrate. Insets illustrate a different rotation angle around a vertical z-axis. The orientations of the x- and y-axes are given approximately for eye guidance. In (A and B) the scale bars are 30 nm. The NSs were incubated for 24 h in the DMF-water mixture at C_w=4 vol. % at 40 ^oC.

1.6 Control experiments

Control experiments conducted in good solvent

In control experiments, the 0.3 nM solution of PS-50K-capped gold NSs was maintained at 40 °C for 24 h in DMF (good solvent) without addition of water. Importantly, for control experiments, efforts have been made to reduce the effect of atmospheric humidity, e.g., we used fresh anhydrous DMF from the bottle sealed with a rubber gasket, sealed vials with colloidal solutions with Parafilm and minimized the time of sample exposure to air during handling. Figure S22 shows images of 40 and 60 nm-diameter NSs in control experiments.

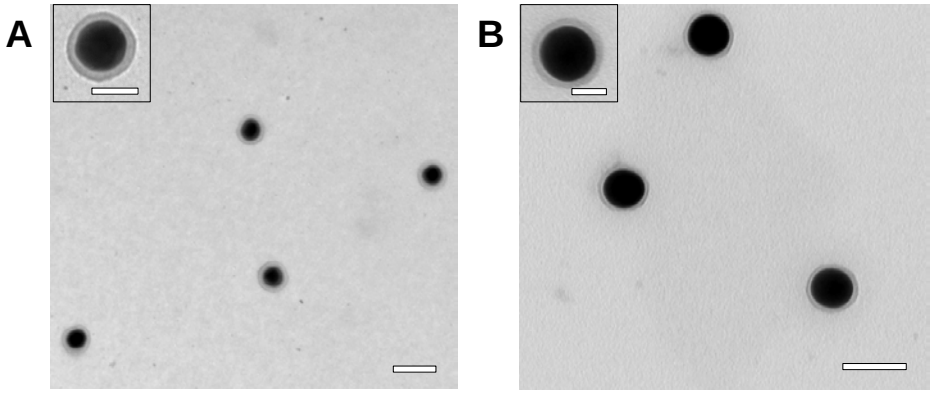

Figure S22. Polymer-capped gold nanospheres in a good solvent. TEM images of 40 nm (**A**) and 60 nm (**B**) diameter gold NSs stabilized with PS-50K and incubated in DMF for 24 h at 40 ^{o}C. Scale bars are 100 nm. Insets show corresponding individual NSs. Scale bars are 40 nm.

Experiments performed at high water content. Polymer surface segregation experiments were conducted for gold NSs in the DMF/water mixture at C_w=10 vol. %, that is, water content was 2.5-fold higher than in experiments described in main text. A 0.3 nM solution of 20 nm-diameter gold NSs in 500 μL of DMF was sonicated for 5 s. Then, 500 μL of a DMF/water mixture at C_w=20 vol. % was added dropwise to the NS solution in DMF under gentle swirling of the vial, to reach the resulting total water concentration C_w=10 vol. % (as opposed to 4 vol. % in typical experiments). The vial was sealed and maintained in a water bath at 40 °C for 24 h. Figure S23 shows that increase in water content in the DMF/water mixture did not qualitatively change the formation of patchy NSs.

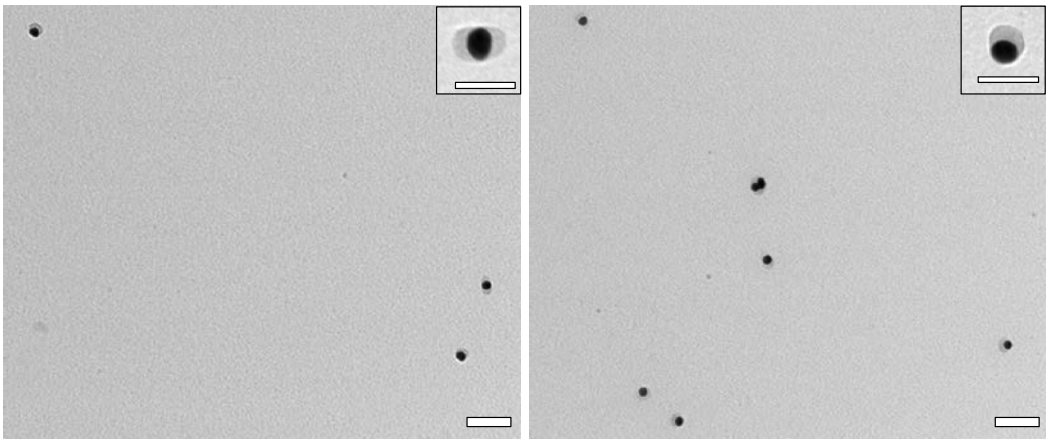

Figure S23. Polymer-capped gold nanospheres in the DMF/water mixture at C_w =10 vol. %. TEM images of gold NSs stabilized with PS-50K. The NSs at the concentration of 0.3 nM were incubated in the DMF-water mixture at C_w=10 vol. % for 24 h at 40 ^oC. Scale bars are 100 nm. Insets show representative single-patch (right) and two-patch (left) gold NSs. Scale bars are 50 nm.

Experiments conducted at high NS concentration. Polymer surface segregation experiments were conducted for gold NSs in the DMF/water mixture at C_w=4 vol. % and NS concentration of 3 nM, that is, ten-fold higher than that described in the main text. A 3 nM solution of 20 nm-diameter gold NSs in 500 μL of DMF was sonicated for 5 s. Then, 500 μL of a DMF/water mixture at C_w=8 vol. % was added dropwise to the NS solution in DMF under gentle swirling of the vial, to reach the resulting total concentration of water C_w= 4 vol. %. The vial was sealed and maintained in a water bath at 40 ° C for 24 h. Figure S24 shows representative TEM images obtained after heating and a histogram of species obtained as determined by TEM imaging. The phase-segregation of PS-50K on the NS surface was qualitatively similar to that occurring in dilute NS solutions, however a larger fraction of NSs formed clusters due to the physical bonding of polymer ligands grafted to different NSs.

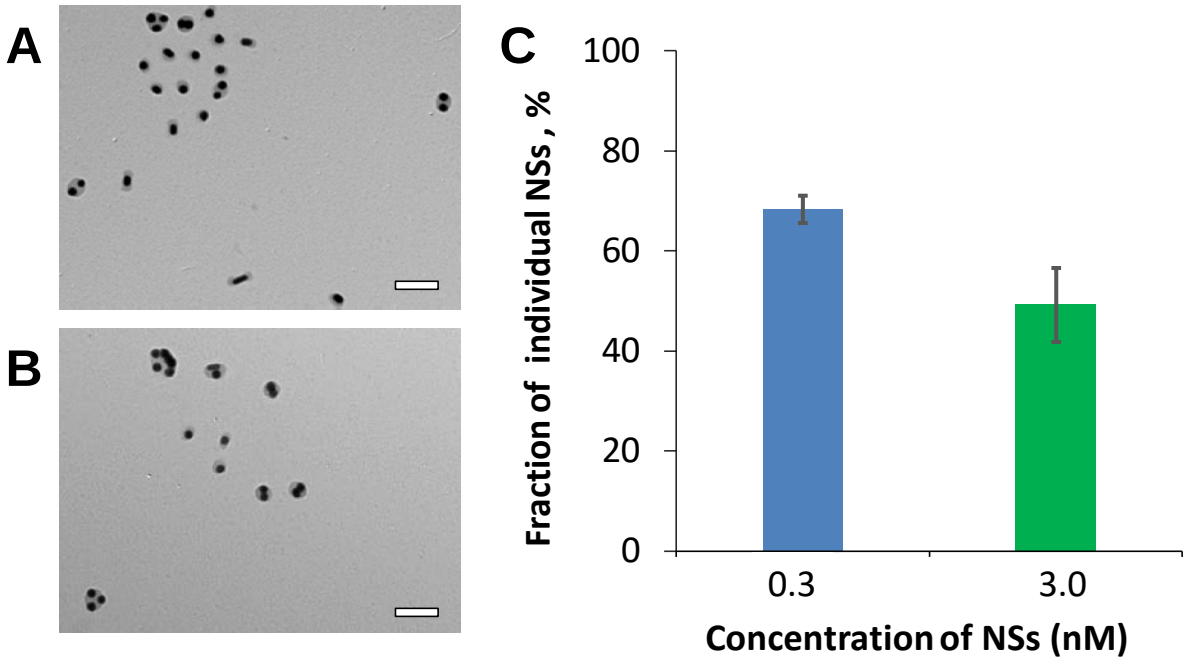

Figure S24. TEM images of polystyrene-stabilized gold nanospheres in the DMF/water mixture. (**A, B**) TEM images of 20 nm-diameter gold NSs stabilized with PS-50K. The NSs were incubated in the DMF-water mixture at C_w=10 vol. % for 24 h at 40 ^oC. The concentration of NSs in the solution was 3 nM. Scale bars are 200 nm. (**C**) Average fraction of individual NSs determined in polymer phase segregation experiments at NS concentration of 0.3 nM (blue) and 3.0 nM (green), based on three series of experiments. In each experiment, 100 species were analyzed. Error bars represent the standard deviation.

Self-assembly of single-patch gold nanospheres

The self-assembly of gold NSs carrying a single patch of PS-50K was examined after their 15 day incubation in the DMF-water mixture at C_w=4 vol. % at 40 ºC (Figure 25A). Isolation of small NS clusters from predominant NS chains was performed by 10 min-long centrifugation

of 1.5 mL of the NS solution at 4,000 *g*. After centrifugation, the top 0.75 mL of the solution was separated from the bottom 0.75 mL above the sediment. Representative images of the top and bottom fractions collected after centrifugation are shown in Figure S25B and C, respectively. The top fraction contained small NS clusters, namely, dimers and trimers, in which the NSs were linked *via* a PS patch (Figure 25B). A network of NS chains imaged prior to centrifugation is shown in Figure 25D. Importantly, dimer and trimer building blocks (highlighted with red and yellow circles, respectively) could be clearly discerned in the short chains and in the network, which suggested two time scales in NS assembly (Figure C and D), suggesting a new, two-step mechanism of NP assembly. First, the patchy NSs assembled in dimers and trimers, due to the efficient binding of PS-50K patches. Then, the dimer and trimer intermediate building blocks assembled into chains, due to the less efficient binding between the NSs surfaces deprived of the polymer.

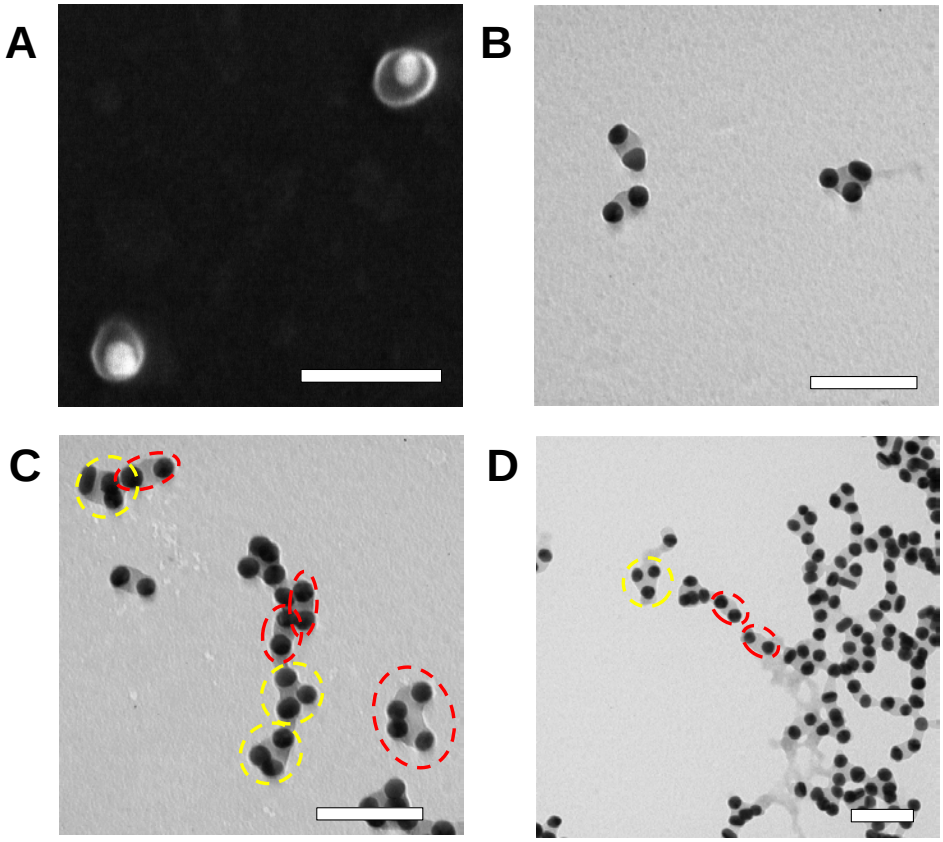

Figure S25. Self-assembly of single-patch gold nanospheres. **A**, SEM image of single-patch gold NSs. **B-D**, TEM images of small clusters ((B), short chains (C) and linear and network structures (D). In (C and D) several dimer and trimer building blocks are highlighted with red and yellow circles, respectively. The structures shown in (B and C) were separated by 10 min centrifugation of 1.5 mL of the NS solution at 4,000 *g* and separation of the top solution (B) and the bottom-level solution (C) (*see text*). The sample in (D) is imaged before centrifugation. The NSs were capped with PS-50 K and incubated in the DMF-water mixture at C_w=4 vol. % at 40 ºC for 15 days. The images are representative of at least, 20 inspected images. Scale bars are 100 nm.

The robustness of the self-assembled chains was examined by 45 min sonication of the solution of patchy NS after its 15 day incubation. Figure S26 shows a representative dark field mode SEM image of the sonicated chains. Inspection of 10 SEM images revealed that the NS chains did not noticeably disintegrate. Dimers of NSs (circled in red color) were clearly recognized in the sonicated structure. Interestingly, the SEM image in Figure 26 shows different modes of the self-assembly of NS dimers, varying from their linear assembly to staggered and side-by-side assembly.

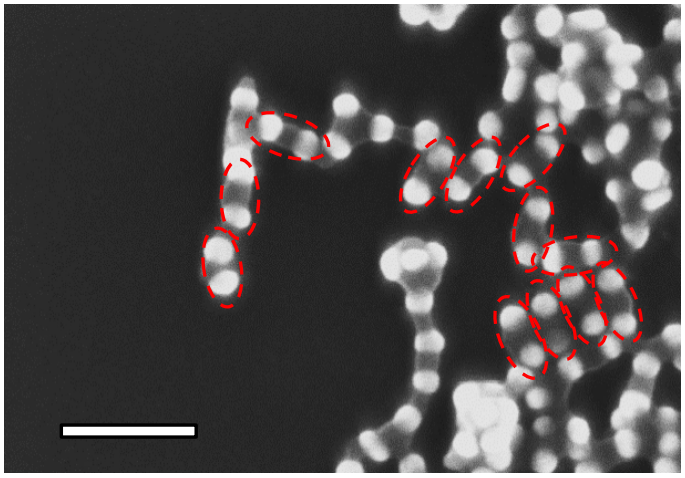

Figure S26. **Dark-field mode SEM image of self-assembled chains of single-patch gold nanospheres following their 45 min sonication**. Gold NSs were capped with PS-50K and incubated in the DMF-water mixture at C_w=4 vol% at 40 ºC for 15 days. Dimers of NPs are highlighted with red circles. Scale bar is 100 nm.

Self-assembly of surface-patterned nanocubes

Exposure of patchy gold NCs overnight to the DMF-water mixture at C_w =4 vol.% at 40 ºC resulted in their self-assembly. Figure S27 A-C shows that surface-patterned NCs formed bonds *via* polymer patches formed at the NC edges (ribs), thus leading to the formation of open structures. In contrast, the NCs uniformly coated with a highly dense polymer layer

(non-patchy NCs) upon their exposure to the DMF-water mixture self-assembled in short chains, with a face-to-face bonding of the NCs to maximize the polymer contact and screen a greater polymer surface area from the poor solvent, in agreement with our earlier work[7]. Figure S27 D-E shows assemblies of silver NCs uniformly coated thiol-terminated polystyrene with a molecular weight 5,000 g/mol. We note that the formation of linear chains, as opposed to three-dimensional clusters, was favored due to the strong contribution of electrostatic repulsion between the NCs at C_w=20 vol. %[17]. As expected, in a good solvent, non-patchy NCs uniformly coated with PS-50K formed close-packed structures with face-to-face NC contacts (Fig. S27F), due to the capillary forces acting between the NCs upon drying.

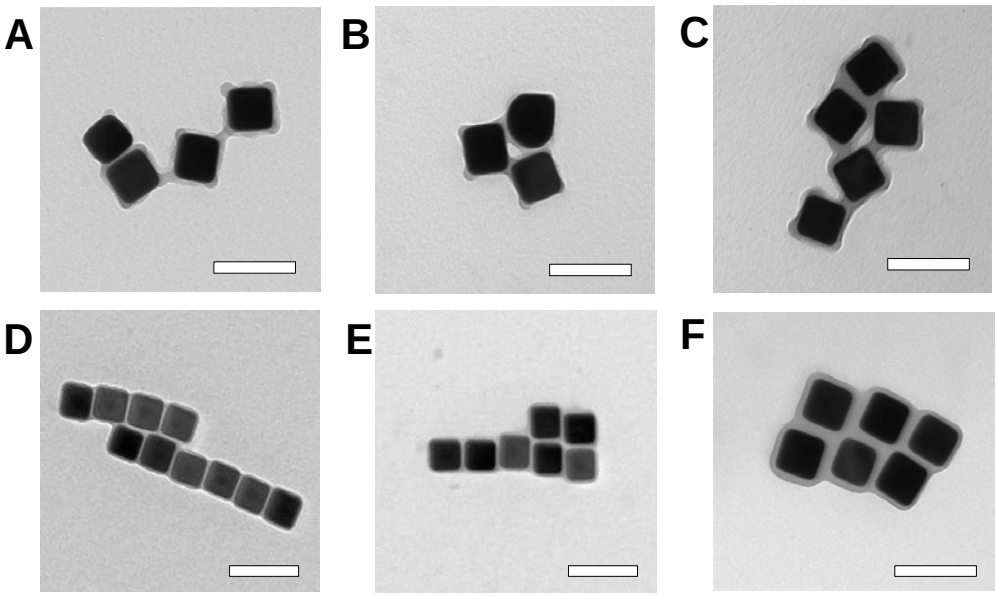

Figure S27. Self-assembly of surface-patterned and non-patterned nanocubes. In A-B and C gold NCs were capped with PS-50K and incubated for 12 h at 40 ºC in the DMF/water solution at C_w=4 vol.%. The ligand exchange procedure was carried out at PS-50K concentration of 0.005 (A, B) and 0.5 mg/mL (C) in THF. Images D-E shows face-to-face assembled chain structures of silver NCs capped with thiol-terminated polystyrene with a

molecular weight 5,000 g/mol after 2 h incubation in the DMF/water solution at C_w=20 vol % at room temperature. In (F) gold NCs uniformly capped with PS-50K and incubated in THF for 12 h at room temperature formed close-packed structures with face-to-face NC contacts. Scale bars are 100 nm.

Self-assembly of patchy gold NSs in the presence of excess polymer

The behavior of patchy NPs as "colloidal surfactants" was explored by examining their self-assembly at the interface between two immiscible liquids (main text, Figure 3H). 250 μL of the mixed solution of gold NSs and non-thiolated (free) polystyrene with a molecular weight 50,000 g/mol in DMF was sonicated for 5 s. The concentration of the NSs and polystyrene were 0.3 nM and 0.25 mg mL^{-1}, respectively. Then, 250 μL of a DMF/water mixture at C_w=8 vol. % was added dropwise to the NS-PS solution in DMF under gentle swirling of the vial, to reach C_w=4 vol. %. The vial was sealed and maintained in a water bath at 40 °C for 24 h and the resulting NS assemblies were subsequently imaged via TEM.

Chain-like assemblies of gold NSs and excess non-thiolated (free) polystyrene (main text, Figure 3H, inset) formed after adding 500 μL of pre-formed single-patch 20 nm-diameter gold NSs functionalized with PS-50K (prepared as described above) to a vial containing 0.03 mg of polystyrene and sonicating the mixture 5 min. Following sonication, the colloidal solution was immediately drop-cast onto a TEM grid.

1.7. Measurement of wetting angle of polystyrene solution on gold surfaces

A 40 μM solution of polystyrene in DMF was prepared. To 500 μL of this solution, 500 μL of 8 vol. % water in DMF was added dropwise to reach the total concentration of water C_W =4

vol. %. After ca. 15 min of stirring, the stir bar was removed and the solution was incubated at room temperature for 48 h. The solution separated into two phases, namely, a solvent-rich phase (the top phase) and a PS-rich phase (the bottom phase). Using a micropipette, 5 μL of the PS-rich phase was deposited onto a silica wafer coated with a 50 nm-thick gold layer. The wetting angle of the PS-DMF-water solution on the gold surface was measured using a DSA-100 Krüss drop-shape analyzer. The average static wetting angle, determined from five independent measurements, was 15.1±0.7º and 12.1±0.4º, for the solution of PS-30K and PS-50K, respectively, which corresponded to a surface tension of 194±49 mN/m for PS-30K and 302± 29 mN/m for PS-50K as determined by drop-shape analysis using a Young-Laplace fit[18].

2. Supplementary Discussion

2.1. Theoretical analysis of the state of the polymer layer on the nanosphere surface in a poor solvent

Consider a nanosphere NS with a diameter D that is capped by flexible polymer molecules end-tethered to its surface with a grafting density σ. Each polymer molecule is composed of $N>>1$ Kuhn segments with a Kuhn length b on the order of the monomer size. The poor quality of the solvent for the polymer ligands is quantified by the dimensionless excluded volume parameter $\tau = (\theta - T)/T$, where T and θ are the theta-temperature and the absolute temperature of the experiment, respectively and $0 < \tau < 1$. An alternative characterization of this poor solvent is given by the size $\xi \approx b\tau^{-1}$ of thermal blobs that attract each other with thermal energy kT, where k is the Boltzmann constant[19]. Since there are τ^{-2} Kuhn monomers per thermal blob, the number of these blobs per molecule is $N\tau^2 > 1$. An isolated polymer

molecule in a poor solvent forms a spherical globule with a radius $R_0 \approx b(N/\tau)^{1/3}$. The surface tension at the polymer-solvent interface of this globule is $\gamma_2 \approx kT\tau^2/b^2$. We assume that the surface tension γ_1 at the NS-solvent interface is equal to the surface tension γ_3 at the NS-polymer interface, giving the contact angle 90^o for the polymer globule on the NS surface, independent of the NS diameter. Polymer volume fraction inside the globule is $\phi \approx \tau < 1$.

Diagram of the states of polymer molecules end-grafted to the nanosphere surface in a poor solvent

Figure S28 shows a theoretical diagram of the states of the polymer end-grafted to the surface of a NS in a poor solvent. Different states of this polymer are described below as different regimes. Experimentally relevant part of the diagram (outlined by a rectangular purple dashed line) is described briefly in the present section and discussed in detail in the following section.

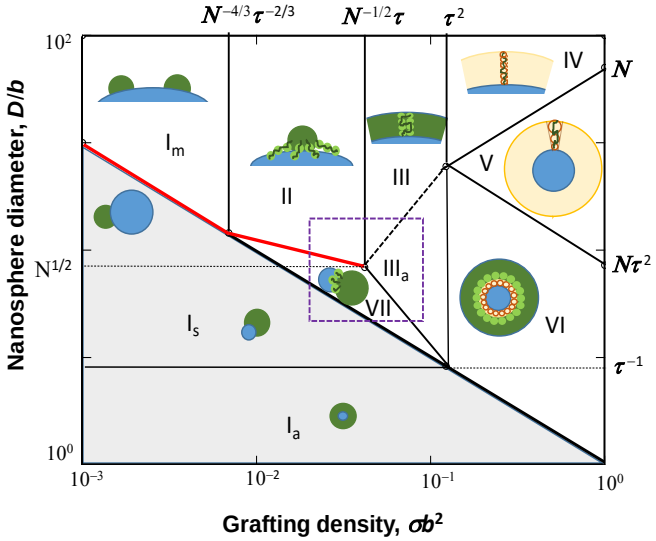

Figure S28. **Theoretical diagram of states of the NS functionalized with end-tethered polymer**. The diagram is plotted in double logarithmic coordinates. Parameters used: N=70, τ

= 0.35, b=1.8 nm, contact angle 90^o. Experimentally relevant part of this diagram is outlined with the dashed rectangle. The cartoons illustrate different states of the polymer on the surface of NSs. .

Regime I_s. The diagonal line with a slope -1/2, described by the equation $\pi D^2\sigma = 1$, gives the condition of grafting single polymer molecule per NS. The regime I_s below this line corresponds to the low grafting density with on average of less than one polymer molecule per NS.

Regime I_m. Above the red section of the diagonal line in the regime I_m, the NSs are capped with more than one chain. At a low grafting density ($\sigma < b^{-2}N^{-4/3}\tau^{-2/3}$), several single-chain polymer globules (patches) do not coalesce, since the stretching energy penalty $kT\tau/(b\sigma^{1/2})$ is higher than the gain in surface energy $kT\tau^{4/3}N^{2/3}$. As a result, grafted polymers form on the NS surface individual globules (patches). The number of globules/NS is $\pi D^2\sigma$. The section of red line with a slope -1/2 between the regimes I_m and I_s corresponds to the boundary between NSs with a different average number of single-chain patches.

Regime I_a. When the NS is smaller than the thermal blob ($D < \xi$), it interacts with segments of polymer molecule with size up to D. These segments are too small to "feel" the poor quality of the solvent. This small NS is fully engulfed with the polymer globule. The boundary between the regimes I_s and I_a corresponds to $D \approx b/\tau$.

Regime II. Groups of P neighbouring tethered molecules segregate into pinned micelles with a core comprising the majority of chain monomers and the stretched micellar legs attaching the core to the NS surface. The average number of pinned micelles (patches) per NS, $\pi D^2\sigma/P$, decreases with decreasing NS diameter D and approaches unity through a cascade of transitions between NS with a different average number of micelles (thick red line

between regimes II and VII).

Regime III. At a higher grafting density $\sigma > \tau/(b^2N^{1/2})$, the pinned micelles merge into a laterally uniform layer with polymer concentration τ. In this regime, the distance between the grafting points $\sigma^{-1/2}$is larger than the thermal blob size $\xi \approx b/\tau$. The thickness of the uniform polymer layer $H \approx b^3N\sigma/\tau$ is smaller than the diameter D of large NS.

Regime III$_a$. Below the dashed line $D = b^3N\sigma/\tau$ with a slope 1, the uniform polymer layer is thicker than the NS diameter. The stretching of the tethered molecules becomes non-uniform and decreases with the distance r from the NS center[20]. The local chain stretching near the NS surface disappears at the boundary $D = \tau/(b\sigma)$ between the regimes III$_a$ and VII. At this boundary, the penalty to form a leg of a pinned micelle (a string of $D\tau/b$ thermal blobs) becomes comparable to the gain in energy due to the formation of the interface between micelle core and NS surface.

Regime IV. At the grafting density of chains $\sigma > (\tau/b)^2$, the distance between the grafting points $\sigma^{-1/2}$ becomes smaller than thermal blob size $\xi \approx b/\tau$ and the grafted polymer chains repel each other *via* three-body interactions. The planar-like θ-brush[21] has the polymer layer thickness $H_\theta \approx bN(\sigma b^2)^{1/2}$, which is smaller than the NS diameter D.

Regime V. The NS diameter D is smaller than the polymer layer thickness, $D < H_\theta$, below the boundary $D = bN(\sigma b^2)^{1/2}$ between the regimes IV and V. The planar layer transforms into a spherical star-like θ-layer with the thickness $H \approx bD^{1/2}(\sigma b^2)^{1/4}N^{1/2}$ and tension decreasing with the distance from the NS center[20]. The outer tension blob becomes equal to the thermal blob at the boundary between the regimes V and VI for $D = N\sigma^{-1/2}\tau^2$.

Regime VI. The polymer layer on smaller NS with $D < N\sigma^{-1/2}\tau^2$ consists of the

collapsed outer sublayer with the thickness $H \approx b[D^2(\sigma b^2)N/\tau]^{1/3}$ and the inner θ-sublayer with the thickness $r_\theta \approx b\sigma^{-1/2}\tau^{-1}D^{-1}$.[20] The θ-sublayer disappears when its thickness becomes comparable to the size of the thermal blob $r_\theta \approx b\tau^{-1}$, which corresponds to the boundary $D \approx \sigma^{-1/2}$ between regimes VI and I_a.

Regime VII. The NS carries a single pinned micelle composed of $\pi D^2\sigma$ molecules for $D < \tau/(b\sigma)$ (below regime III_a) and for $D > \sigma^{-1/2}$ (above regime I_s).

2.2. Theoretical analysis of experimentally relevant polymer states on the nanosphere surface

Figure S29A represents a fragment of the theoretical diagram highlighted with a dashed rectangle in Figure S28, and includes Regimes II, III (including III_a), and VII. At temperature T, the polymer separates from the solvent into a relatively dense phase with the polymer volume fraction $\phi \approx \tau$, where τ is the dimensionless excluded volume parameter of the polymer[19]. The diagram plotted in the σ-D coordinates contains two regions, namely, a pinned micelle regime II (patchy NSs) and a smooth shell regime III (core-shell NSs), which are separated from each other with a blue boundary line. The cartoons in Fig. S29A illustrate NSs with a different number of surface patches.

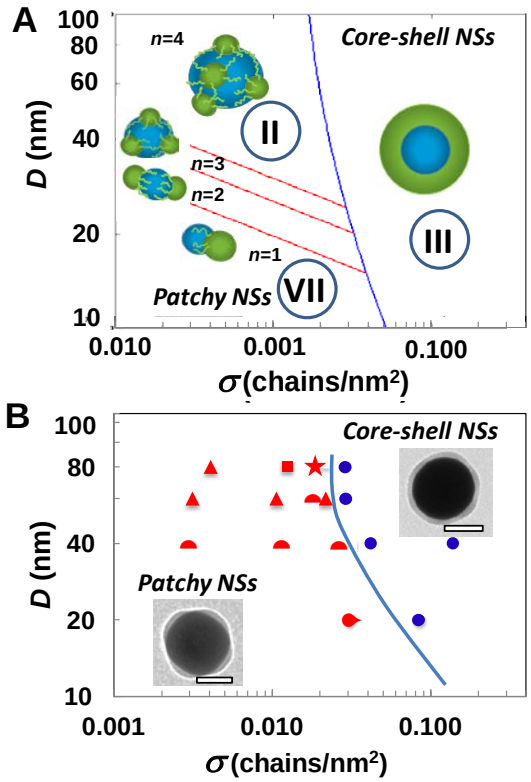

Figure S29. Theoretical and experimental diagrams of states of polymer-grafted nanospheres. (**A**) A theoretical diagram of states of polymers grafted with density σ to the surface of a NS with diameter D. The upper right part of the diagram (regime III for high σ and large D) corresponds to core-shell NSs. The rest of the diagram (regimes II and VII) represents pinned micelles with the number n of micelles per NS increasing from the bottom right to the top left of the diagram. The dark-blue line (eq. S11) shows the boundary between the NSs with a smooth polymer layer (regime III) and patchy NSs (regimes II and VII). Red lines (eq. S9) indicate cascade of transitions between the NSs with a different number n of pinned micelles. The cartoons illustrate NSs with a different number of surface patches. (**B**) Experimental diagram of states of gold NSs tethered with PS-50K, plotted in the D-σ coordinates. The dark-blue boundary line outlines conditions, at which core-shell NSs (●)

and NSs with 5 (★), 4 (■), 3 (▲), 2 (◓) and 1 (◔) patches are formed. Insets show a core-shell NS (σ=0.03 chains/nm^2) and a patchy NS (σ=0.002 chains/nm^2).

Right region of the state diagram (Regime III). At high grafting densities σ (to the right of the boundary line), the grafted polymer chains are stretched to a height exceeding the unperturbed size of the polymer molecule, $R=bN^{1/2}$, where N is the number of Kuhn segments of size b per polymer chain[19]. Deviations of the shape of this layer from a smooth spherical shell are unfavorable, because they increase the area of the polymer-solvent interface in a poor solvent and thus the interfacial energy of the system. Such deviations also increase the polymer stretching free energy[22]. As a result, the dense polymer phase forms a uniformly thick shell around the NS.

Transition between the right and left parts of the diagram. Next, we consider the effect of NS dimensions on the transition between the smooth layer and the pinned micelle regimes. For large NSs ($D >> R$), the transition occurs at polymer grafting density

$$\sigma \approx \tau/(bR) \quad \text{(S3)},$$

at which the layer thickness is comparable to an unperturbed polymer size R. For large NSs, at a lower σ, the polymer molecules in the layer are no longer extended. To reduce the interfacial energy, the condensed polymer phase undergoes dewetting, that is, the segregation of the smooth layer into small droplets (corresponding to the cores of pinned micelles). This effect results in the exposure to the solvent of the NS surface with a lower NS-solvent interfacial tension γ_1 than the tension[19] $\gamma_2 \approx kT\tau^2/b^2$ of the polymer-solvent interface. The dewetting is constrained, because the polymer molecules (micellar "legs") are strongly surface-tethered and have to stretch to reach micellar cores.

Each pinned micelle is composed of P chains, with the micellar core comprising the major fraction of each polymer molecule, and P legs. The aggregation number P of the micelles is determined by the balance of the surface free energy per polymer chain ~ $\gamma_2 R_c^2/P$ of the micellar core of radius R_c and the free energy of stretched legs. The average length of a leg is given by the radius $A^{1/2} \approx (P/\sigma)^{1/2}$ of a footprint area A of the micelle. The stretching energy of the leg can be estimated as $kT(P/\sigma)^{1/2}\tau/b$, that is, the ratio of the leg length and a characteristic tension length scale b/τ, dependent on the quality of the solvent. Since the micellar core has the same polymer volume fraction $\phi \approx \tau$ as the dense polymer phase, its radius R_c is related to the aggregation number P as $R_c \approx b(NP/\tau)^{1/3}$. The balance of the interfacial free energy per polymer chain in the core, $\gamma_2 R_c^2/P$ ($\approx kT\tau^2(NP/\tau)^{2/3}/P$) and the free energy of leg stretching, $kT(P/\sigma)^{1/2}(\tau/b)$, determines the micellar aggregation number of large NSs in a quasi-planar regime[23].

$$P \approx N^{4/5}(\sigma b^2)^{3/5}\tau^{2/5} \qquad \text{(S4)}$$

The incline of the blue boundary for the NSs with large but finite diameters $D > R$ is governed by the curvature-induced increase of the area of polymer-solvent interface per chain with a decreasing NS diameter at σ = const, that is, from $1/\sigma$ per chain to $(1+2H/D)/\sigma$ per chain, where H is the thickness of the polymer layer. The corresponding increase of the surface free energy per chain $2\gamma_2 H/(D\sigma)$ destabilizes the uniformly thick polymer shell. At a particular grafting density σ and decreasing NS diameter D, this effect is stronger than the increase of free energy of micellar legs, due to their extra-stretching proportional to $1/D^2$. Therefore, a uniformly thick polymer layer on smaller NSs is destabilized at larger values of σ, thus resulting in the incline of the blue boundary in Fig. S29A for $D > R$ toward larger grafting density

$$\sigma \approx \frac{\tau}{b}\left(\frac{1}{R}+\frac{2}{D}\right) \quad \text{(S5)},$$

where the sum in the parenthesis is the sum of the reciprocal chain size *1/R* and the reciprocal NS radius *2/D*.

Left region of the state diagram (Regimes II and VII). At a lower grafting density σ (to the left of the blue boundary line), the NSs are covered by pinned micelles. The number of pinned micelles

$$n \approx \frac{D^2\sigma}{P} \approx \left(\frac{D}{b}\right)^2 \left(\frac{\sigma b^2}{\tau N^2}\right)^{2/5} \quad \text{(S6)}$$

and the micellar size (footprint diameter) $(P/\sigma)^{1/2}$ are not strongly affected by the NS curvature, as long as $D >> (P/\sigma)^{1/2}$. This condition is equivalent to $n >> 1$, that is, a large number of micelles per NS for

$$D >> bN^{2/5}\,[\tau/(\sigma b^2)]^{1/5} \quad \text{(S7)}$$

A decrease in *D* leads to the decrease in the total number, *n*, of pinned micelles per NS (Eq. S6) without a noticeable change in their equilibrium aggregation number *P*, as long as $n >> 1$. Transitions between the NSs with a different integer number *n* of pinned micelles are illustrated by the series of red lines in the diagram in Fig. S29A. Each of these lines between NS states with *n* and *n* +1 micelles is described by the relation

$$D \approx \left[\left(n+\frac{1}{2}\right)\frac{P}{\sigma}\right]^{1/2} \quad \text{(S8)}$$

Using eq. S4 for equilibrium aggregation number, *P,* one obtains the expression for the red transition lines in Fig. S29A

$$D \approx \left(n+\frac{1}{2}\right)^{1/2} bN^{2/5}\left(\frac{\tau}{\sigma b^2}\right)^{1/5} \quad \text{(S9)}$$

The transition between a single-patch and two-patch NS (that is, a NS with one and two pinned micelles, respectively) is illustrated in Fig. S30. The transition occurs when the legs of a single-patch NS are over-stretched, while the legs on a two-patch NS are not sufficiently stretched to balance interfacial energy of micellar core.

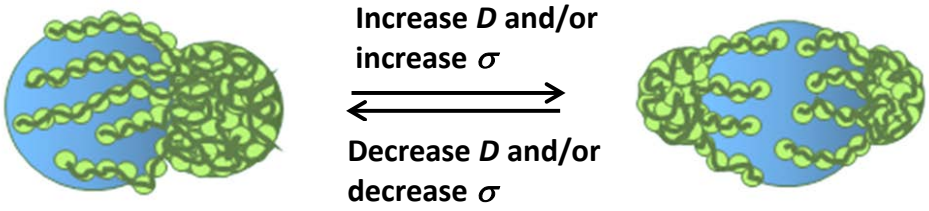

Figure S30. Schematic of the transition between a single-patch and a two-patch nanospheres. The NSs coexist at the transition line (eq. S9) with n=1. Polymer chains are shown by dark green.

In Fig. S29A, below the lowest red line (corresponding to a single pinned micelle per NS, n = 1), the decrease in D leads to the reduction in the total number ~ $D^2\sigma$ of tethered chains and the corresponding micelle aggregation number $P \approx D^2\sigma$. The surface free energy gain due to partial NS wetting by the micelle core (compared to the complete NS wetting with a laterally homogeneous layer) decreases as $\gamma_2 D^2$. This gain is balanced by the free energy loss of $kTD\tau/b$ per stretched leg. For small NSs at $D < R$, the position of the blue line in Fig. S29A is determined by the balance of the interfacial surface energy ~ $\gamma_2 D^2 \approx kT\tau^2 D^2/b^2$ and the free energy of $D^2\sigma$ stretched legs losing ~ $kTD\tau/b$ per leg. This boundary between the laterally smooth layer (regime III) and the single pinned micelle regime VII is given by

$$D \sim \tau/(b\sigma) \quad \text{(S10)}$$

with a slope of *-1* on a double-logarithmic scale in the right lower part of the diagram in Fig. S29A, consistent with eq. S5 for $R>>D$. Therefore, the equation for the blue boundary in Fig. S29A given by eq. S5 can be rewritten as

$$D \approx \frac{2}{\frac{b\sigma}{\tau}-\frac{1}{R}} \quad \text{(S11)}$$

Although the scaling-type diagram of states in Fig. S29A was constructed for a polymer-NS contact angle of 90^o, it is expected that the main features of the diagram would hold for smaller contact angles reported in Section 1.7.

Comparison of the experimental and theoretical diagrams of NS states. The experimental state diagram plotted in Fig. S29B reproduced all essential features of the theoretical diagram (Fig. S29A), including the transition between the patchy NSs and core-shell NSs. Both diagrams underlined that for small NSs (larger curvature) the transition occurred at higher grafting densities than for large NSs. This trend is reflected by the negative slope of the blue boundary line at small values of D and high values of σ. By inserting the experimental value of τ =0.35 for the DMF/water mixture at $C_{w=}$4 vol. %[24], Kuhn length[19] b=1.8 nm[19], chain size R=15 nm and without any adjustable parameters in eq. S11, the shape and the position of the boundary line between the patchy and smooth-shell NSs was reproduced (see blue lines in Figs. S29A and B).

For small and intermediate values of σ, the number of patches per NS, n, increased with increasing NS dimensions. For a particular value of D, no obvious variation of n *vs.* σ was observed, with an exception of 80 nm-diameter NSs for which n decreased with reducing

σ (as predicted by eq. S6). The transitions shown with red lines in Fig. S29A were obtained by inserting τ=0.35, *b*=1.8 nm, *N*=70 without using any adjustable parameters in eq. S9.

3. References and Notes

1. Jana, N. R., Gearheart, L., Murphy, C. J. & Carolina, S. Seeding growth for size control of 5-40 nm diameter gold nanoparticles. 6782–6786 (2001).

2. F.-R. Fan *et al.*, Epitaxial growth of heterogeneous metal nanocrystals: from gold nano-octahedra to palladium and silver nanocubes. *J. Am. Chem. Soc.* **130**, 6949–6951 (2008).

3. F. Lu *et al.*, Discrete nanocubes as plasmonic reporters of molecular chirality. *Nano Lett.* **13**, 3145–3151 (2013).

4. R. Zou *et al.*, Selective etching of gold nanorods by ferric chloride at room temperature. *CrystEngComm*. **11**, 2797–2803 (2009).

5. X. Ye, C. Zheng, J. Chen, Y. Gao, C. B. Murray, Using binary surfactant mixtures to simultaneously improve the dimensional tunability and monodispersity in the seeded growth of gold nanorods. *Nano Lett.* **13**, 765–771 (2013).

6. Grzelczak, M. et al. Steric hindrance induces crosslike self-assembly of gold nanodumbbells. Nano Lett. 12, 4380–4384 (2012).

7. Klinkova, A. *et al.* Structural and optical oroperties of self-assembled chains of plasmonic nanocubes. *Nano Lett.* **14,** 6314–6321 (2014).

8. Chen, H. et al. Plasmon coupling in clusters composed of two-dimensionally ordered gold nanocubes. *Small* **5**, 2111–2119 (2009).

9. S. K. Varshney, X.-F. Zhong, A. Eisenberg, Anionic homopolymerization and block

of 4-vinylpyridine and its investigation by high-temperature size-exclusion chromatography in *N*-methyl-2-pyrrolidinone. *Macromolecules* **26**, 701–706 (1993).

10. C.-F.Huang, J. A.Yoon, K. Matyjaszewski, Synthesis of *N*-vinylcarbazole-*N*-vinylpyrrolidone amphiphilic block copolymers by xanthate-mediated controlled radical polymerization. *Can. J. Chem*., **88**, 228–235 (2010).

11. G. Moad, E. Rizzardo, S. H. Thang, Living radical polymerization by the RAFT process. *Aust. J. Chem.* **58**, 379–410 (2005).

12. D. L. Patton, M. Mullings, T. Fulghum, R. C. Advincula, A facile synthesis route to thiol-functionalized α, ω-telechelic polymers via reversible addition fragmentation chain transfer polymerization. *Macromolecules* **38**, 8597–8602 (2005)

13. Gold Nanoparticles: Properties and Applications (Sigma-Aldrich technical report; http://www.sigmaaldrich.com/materials-science/nanomaterials/gold-nanoparticles.html).

14. M. C. Costache, C. A. Wilkie, High-throughput method for estimating the time to sustained ignition of polystyrene-clay nanocomposites based on thermogravimetric analysis. *Polym. Adv. Technol.* **21**, 506–511 (2010).

15. N. Benoit *et al.*, Measuring the grafting density of nanoparticles in solution by analytical ultracentrifugation and total organic carbon analysis. *Anal. Chem.* **84**, 9238–9245 (2012).

16. W. M. Haynes, Ed., *CRC Handbook of Chemistry and Physics*. (CRC Press, Boca Raton, FL, ed. 95, 2014).

17. Choueiri, R. M., Klinkova, A., Thérien-Aubin, H., Rubinstein, M. & Kumacheva, E. Structural transitions in nanoparticle assemblies governed by competing nanoscale forces. *J. Am. Chem. Soc.* **135,** 10262–10265 (2013).

18. H.-J. Butt, K. Graf, M. Kappl, *Physics and Chemistry of Interfaces*. (Wiley, 2003).

19. Rubinstein, M. & Colby, R. H. *Polymer Physics*. (Oxford University Press, 2003).

20. E. B. Zhulina, O.V. Borisov & T. M. Birshtein, Coil-globule transition in star-like macromolecules. *Polym. Sci. U.S.S.R.* **30,** 780–788 (1988).

21. E. B. Zhulina, O. V. Borisov, & V. A. Priamitsyn, Theory of steric stabilization of colloid dispersions by grafted polymers. *J.Colloid Interf. Sci.* **137**, 495–511 (1990).

22. F. J. Solis, G. T. Pickett, On the stability of the Alexander polymer brush. *Macromolecules* **28**, 4307–4312 (1995).

23. E. B . Zhulina, T. M. Birshtein, V. A. Priamitsyn. & L. I. Klushin, Inhomogeneous structure of collapsed polymer brushes under deformation. *Macromolecules* **28**, 8612–8620 (1995).

24. Z. Nie, *et al.* Self-assembly of metal-polymer analogues of amphiphilic triblock copolymers. *Nat. Mater.* **6,** 609–614 (2007).